THE EFFECT OF PROFESSIONAL BALLET TRAINING ON BRAIN STRUCTURE: A TALE OF TWO FRACTIONAL ANISOTROPY METRICS

CHARLES S. LEGER

A THESIS SUBMITTED TO
THE FACULTY OF GRADUATE STUDIES
IN PARTIAL FULFILLMENT OF THE REQUIREMENTS
FOR THE DEGREE OF
MASTERS OF ARTS

GRADUATE PROGRAM IN PSYCHOLOGY
YORK UNIVERSITY
TORONTO, ONTARIO

OCTOBER, 2014

Abstract

This research investigated structural brain changes associated with long-term professional ballet dance training. The primary measure used was fractional anisotropy (FA), a diffusion tensor (DTI) derived index of water molecule diffusion, which putatively quantifies main neural tract efficiency. Dancers had higher FA (p = .062, FWE corrected), which ostensibly reflects greater axonal ability to communicate. Dancers also had differing FA lateralization (p = .038, FWE corrected). Large percentages (30% to 55%) of variability in these metrics were shared by years of dance training, implicating a substantive impact of dance training on brain structure. Other DTI-derived indices where used to help characterize FA (i.e. axial diffusion, radial diffusion, and mean diffusion), and the results implicate enhanced conduction from altered tract properties, perhaps increased myelination. In addition, dancers had greater global grey matter and white matter volume, large percentages in the variability of which were also shared by years of training.

ACKNOWLEDGEMENTS

This thesis would not have been possible without the inspiration and support of my supervisor Joseph DeSouza. I would also like to thank Tuan Cao-Huu (Glendon Campus) who, on very short notice, kindly accepted the role of advisor. In addition, lab associates Samantha Leung and Paula Di Noto were extremely helpful in providing supportive study data.

TABLE OF CONTENTS

LIST OF TABLES

LIST OF FIGURES

Chapter One

Introduction

1.1 Diffusion Imaging Metrics and the Diffusion Tensor Model

The human brain has known structural asymmetries including the common human macrostructural trait of the left frontal lobe and right occipital lobe patelias (in most individuals the left frontal and right occipital lobes are larger than the contralateral counterparts) (Kennedy et al., 1999); gross age-related perisylvian sulcal asymmetry, where adults show greater perisylvian asymmetry than children (Sowell et al., 2002); and neuroanatomical asymmetry, language being a much studied example (Damasio & Geschwind, 1984). The advent of diffusion magnetic resonance imaging (DTI) has facilitated analysis of brain asymmetries, particularly of white matter asymmetries, by a variety of methods (e.g. tractography, volumetric segmentation, mean diffusivity, FA, etc.). The structural asymmetric properties of the brain are frequently characterized in research by DTI-derived FA analysis. Many studies assess FA asymmetry of tracts or regional structures, others investigate T1-derived GM and WM volumetric asymmetry (mainly GM), while yet others studies use a combination of metrics.

It is neurologically normal and virtually invariant for specific major fiber tracts to connect different regions of the brain: e.g. SLF connects the frontal and posterior hemispheres; the uncinate fasciculus connects the temporal and frontal areas; the corpus callosum connects the two hemispheres (Huettel, Song, & McCarthy, 2009; Nolte, 2009). However, the integrity of these connections and that of the multiplicity of other tracts varies between individuals. Development, aging and pathologies can dramatically alter neural tract microstructure (Horsfield & Jones, 2002; Lim and Helpern, 2002; Neil et al., 2002; Pagani et al., 2005). Of greater relevance to this investigation, training and expertise have been reported associated with altered macrostructure (e.g. GM volume), altered microstructure (e.g. FA), or a mixture of macro and microstructural changes (Bengtsson et al., 2005; Boyke, Driemeyer, Gaser, Buchel, & May, 2008; Draganski et al., 2004; Driemeyer, Boyke, Gaser, Buchel, & May, 2008; Halwani, Loui,

Ruber, & Schlaug, 2011; Hanggi, Koeneke, Bezzola, & Jancke, 2010; Imfeld, Oechslin, Meyer, Loenneker & Jancke, 2009; Ilg et al., 2008; Keller & Just, 2009; Koeneke, Hoppe, Rominger, & Hanggi, 2009; Nigmatullina, Hellyer, Nachev, Sharp, & Seemungal, 2013; Schmithorst & Wilke, 2002; Scholz, Klein, Behrens, & Johensen-Berg, 2009; Takeuchi et al., 2010, Taubert et al., 2010). Such experience-dependent changes are most demonstrative of the neuroplastic property of the brain (Pascual-Leone et al., 2005). It must be underlined that alterations in function frequently stem from tract rather than cortical gray matter alterations (Rudrauf, Mehta, & Grabowski, 2008) emphasizing that connectivity constrains function.

Magnetic resonance diffusion tensor imaging (DTI) is recognized as a highly sensitive indicator of microstructural changes in tissue, especially brain white matter (WM) neural tracts. DTI is (typically) a pulsed-gradient spin-echo sequence (PGSE) of externally applied magnetic gradients that provide magnitude and direction measures of water molecule diffusion in the brain. In the commonly used diffusion tensor model (Fig. 1), each tensor includes eigenvectors V1, V2, and V3 that are perpendicular to each other in Cartesian x, y and z fashion. The eigenvalues λ1, λ2, and λ3 describe the length of V1, V2 and V3 eigenvectors. Diffusion along the main axis is termed axial diffusivity (AD) or λ1; radial diffusivity (RD) occurs perpendicular to the main axis of diffusion and is the average of eigenvalues λ2, and λ3 (λ2 + λ3/2). The assumption is made that the main direction or more precisely the orientation of diffusivity is an estimate of underlying tract (axon) orientation (Pierpaoli & Basser, 1996). Restriction of water molecule diffusion is not uniform in all directions; diffusion progress is more restricted across than along tracts. Such diffusion, then, is ostensibly affected by the microstructure of underlying tissue.

Two of the most commonly used DTI metrics of microstructural status and change are mean diffusivity (MD) and FA. MD refers to isotropic-type diffusion, which is equivalent in all directions. The elements of such diffusion result in a circular dispersion pattern. MD is highest in regions with the least restriction such as the cerebral spinal fluid. It is defined by the equation $MD = \lambda 1 + \lambda 2 + \lambda 3/3$. By contrast, FA describes anisotropic diffusion; a diffusion pattern characterized by ellipsoid dispersion (Huttel, Song, & McCarthy, 2008; Sotiropoulus & Anderson, 2014) that indicates a preferred direction of diffusion; it

ostensibly quantifies the extent of underlying local tract structure directionality. It is widely defined by the equation $FA=\sqrt{3}/2\sqrt{\sum(\lambda i - (\lambda)^2 / \sum \lambda i^2}$, where i =1, 2, 3 (λ1, λ2, λ3). In essence, FA is a measure of water diffusion variability; variability that is assumed to characterize underlying tract structure integrity (Smith et al., 2006). High directionality or anisotropy approaches 1, while low anisotropy approaches 0 ($0 \leq FA \leq 1$). Diffusion is facilitated along the main axis of a fiber bundle (V1) but hindered along an axis perpendicular to the main fiber bundle (Moseley et al, 1990). Relative diffusivity is associated with the degree of myelination (Beaulieu 2002; Song et al., 2005) and FA has been reported to generally increase with age from birth to 18 years of age (Verhoeven et al., 2010). In diffusion-weighted imaging, statistical variations in anisotropy are color/brightness coded and depend on both the duration and strength of applied magnetic gradients as well as the strength of diffusion directionality (see Figure 1).

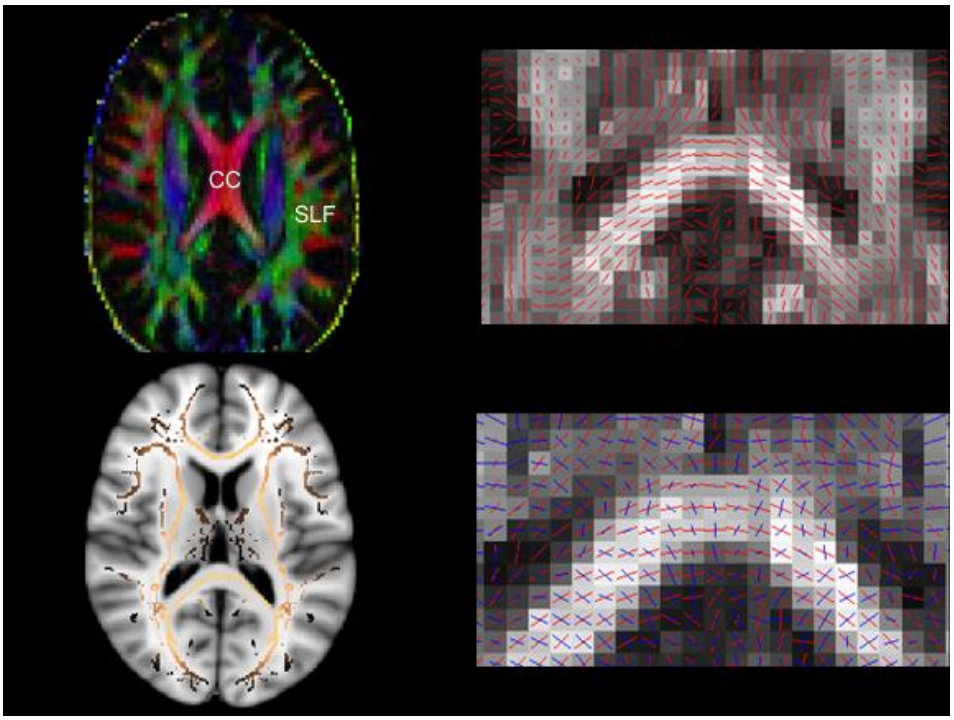

Figure 1. FA color map, top left; V1 top right; symmetrised FA skeleton lower left; V1 (red) and perpendicular V2 (blue)

Of note, the pattern of reduced FA but increased MD within neural tracts can be an indication of axonal damage and vasogenic edema (Charlton et al., 2006; Kim & Jang 2013). The dual microstructural indices

of AD and RD have been used to help understand FA change mechanisms (Metwalli et al., 2010; Tang, Lu, Fan, Yang, & Posner, 2012; Wheeler-Kingshott & Cercignani, 2009). It is expected that higher FA would be associated with greater AD while lower FA would be associated with greater RD (Beaulieu, 2002). Moreover, antithetical implications of FA and RD can be gleaned from longitudinal data. Between 6 and 68 years of age, and within the main white matter brain pathways, FA and RD show opposite distribution shapes: RD follows a U-curve with progressing age while FA follows an inverted U-curve (Hasan et al., 2010). Quite simply, the FA value can be due to a relative increase in AD, a relative decrease in RD or both.

There is typically high homogeneity of structural fiber orientation in parts of several main neural tracts (corpus callosum, cingulum, the SLF etc.). This is illustrated in top right image of Figure 1: the red lines of the vector field (V1) are generally aligned with the underlying (hat-shaped) aspect of the corpus callosum (normally a region of relatively high FA). Tractography connects the preferred direction of vectors to form streamlines or pathways. However, with over a billion neurons, and the axons of many exceeding 15cm in length, connectivity in the massive network that is the brain is complex; tracts fan-out and intersect frequently. Further, it has been estimated that at least 2 different fiber tracts with non-parallel orientations cross in about 1/3 of voxels (Tuch, Weisskoff, Belliveau, & Wedeen, 1999). Returning to Figure 1, this too is represented where the main (hat-shaped) segment of the corpus callosum intersects with other tracts; the vector orientations of such crossing tract areas are clearly heterogenic. When multiple tracts pass through a voxel, as would be expected where tracts cross, multiple intra-voxel fiber orientations result which can't be individually resolved with the tensor model; the tensor model's single main eigenvector (V1) can infer only a single primary direction of diffusion (Tuch, 2002). As such, a general criticism of the diffusion tensor model is its assumption of homogeneity of axon orientation- the assumption of a Gaussian tract distribution within a voxel.

To resolve and separate intersecting tracts within a voxel and infer the directions of maximal diffusivity (maximal FA) high angular resolution diffusion imaging (HARDI) was developed (Tuch et al., 1999; Tuch, 2002). The HARDI method of inferring tract orientation was pioneered by Tuch et al. (1999)

and involves the orientation distribution function (ODF). ODF is a mixture of finite Gaussians that solves for eigenvectors with the smallest error between observed and predicted diffusion signals (for details see Tuch, 2004). Several methods that use HARDI have been developed to infer heterogeneous fiber directions (Alexander, 2005; Özarslan & Mareci, 2003; Özarslan et al., 2006: Wedeen, Hagmann, Tseng, Reese, & Weisskoff, 2005). For a review of HARDI acquisition analysis methods, see Barnett (2009). In general, HARDI is an unquestionably valuable acquisition method but it is computationally expensive and requires greatly extended scanning times to acquire the necessary data. In addition, one of the most used HARDI image processing methods, known as q-ball imaging, has been demonstrated to yield a poor level of ODF accuracy (Barnett, 2009).

Tract-based spatial statistics (TBSS; Smith et al., 2006), (part of FMRIB's software library v5.0, http://fsl.fmrib.ox.ac.uk/fsl/fslwiki), approach to voxel heterogeneity in diffusion data analysis includes the use of a mean FA "skeleton" (shown in Figure 1, lower left image) which reduces comparisons and hence family wise errors (FWE) as well as extremes making the distribution more Gaussian. Of greater import in this regard, is the non-parametric permutation approach adopted which relaxes the Gaussian requirement for tensor model data. For example, the test statistic of choice (usually a t-test on a cluster of voxels) can be tested against the null distribution values of randomly permuted data across the entire FA skeleton (Smith et al., 2006).

1.2 Anatomical landmarks of brain asymmetry

Leftward SLF asymmetry (L > R) epitomizes lateralization, and SLF research is extensive. Our engagement in language tends to be strongly leftward lateralized mainly within the frontal and temporal areas connected by SLF fibers. Classically, language has been described as a function of the SLF-linked Wernicke – Broca neuroanatomy (Geschwind & Levitsky, 1968). By contrast, our sense of location and spatial orientation tends to be rightward lateralized, and dominated by the right parietal cortex (Carlson, 2008), and disruption of a right temporoparietal element – the right supramarginal gyrus (SMG) - by transcranial magnetic stimulation (TMS) was recently found to impair perception of spatial orientation (Kheradmand, Lasker & Zee, 2013). Components of the SLF association bundle serve both these

asymmetries: Wernicke-Broca connectivity is largely served by the AF portion of the SLF, an inferior aspect of the SLF (SLF-IV) also referred to as the direct SLF segment (Catani et al., 2005). Fibers of the superior portion of the SLF serve the angular (SLF-II) and supramarginal (SLF-III) gyri of the parietal cortex (Makris et al., 2005).

Both the SLF and cingulum are regarded as among the most prominent of association fibers; they are bi-directional, and fan-out throughout their course (Nolte, 2008). The cingulum is a medial limbic system component that courses within the cingulate gyrus and surrounds the corpus callosum. Its long fibers run between the temporal and frontal lobes, the longest of which courses between the anterior temporal and orbitofrontal cortices. Its shorter fibers connect aspects of the cingulate cortex as well as medial occipital, parietal, temporal and frontal areas (Catani et al., 2008). Left and top view reproductions of the cingulum are shown in Figure 2. Probabilistic tractography has shown that lesions of the left cingulum (hippocampal processes) but not right cingulum impair visuospatial processing (Rudrauf et al., 2008).

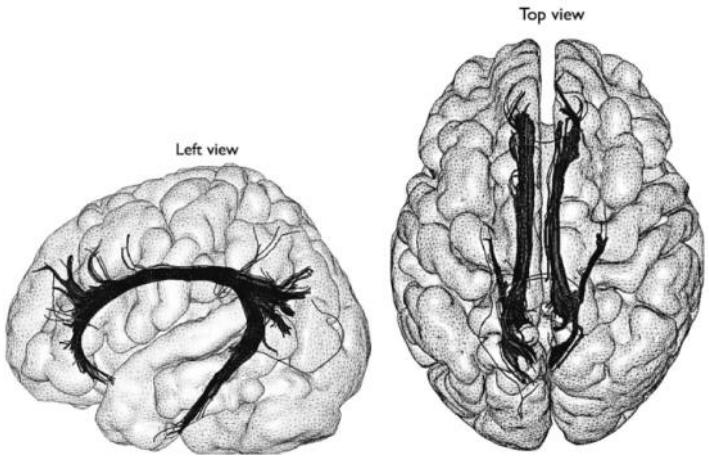

Figure 2. The left view shows the U-shaped configuration of the cingulum fibers connecting the cingulate cortex regions and medial aspects of the occipital, parietal, temporal and frontal lobes. The top view

shows the medial positioning and anterior- posterior expanse of the cingulum. Reprinted from Catani et al., (2008)

The SLF courses between frontal and posterior hemispheres above the insula; it fans out at the occipital, parietal and temporal lobes. But the anatomy of the SLF has been further refined, with the conventionally designated AF as the primary but not only component of the SLF. Differing parcellations of the SLF are depicted in Figures 3 (Makris et al., 2005) and 4 (Catani et al., 2007). The SLF long direct segment is frequently also referred to as the AF and it has been most often depicted (e.g. in tractography) as the dominant language pathway (see Figure 3, color-coded red), and as exclusive to the left hemisphere (Catani et al., 2007).

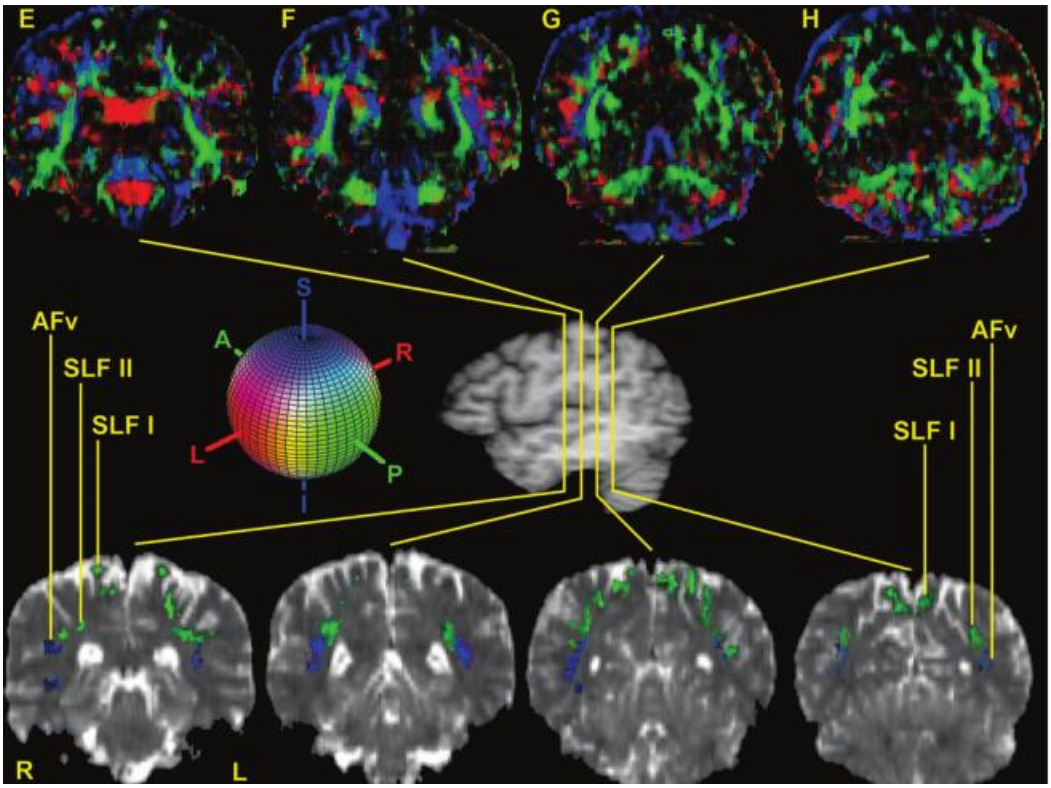

Figure 3. The lower rows (T2-weighted EPI images) show the topographical locations of the SLF subcomponents. SLF-I (corresponds to the anterior indirect segments of Catani et al. (2005 [color-coded green in Figure. 4]), SLF-II, and SLF-III (green) run anterior-posterior; the arcuate (AFv) seen in the middle frame (blue) runs mostly inferior-superior (contrary to the more traditional tractography

reconstruction of the arcuate long direct segment depicted in red in Figure 4 connecting Wernicke's and Broca's areas exclusively in the left hemisphere. Reprinted from Makris et al. (2005).

In a variation of the conventional AF configuration, research by Makris et al. (2005) characterized the AF orientation (virtually a z-direction rather than y-direction) and termination differently . The deterministic tractography findings of Bernal et al. (2010) support the Makris model: AF rostral end projections points fell in the precentral gyrus, not reaching Broca's area in 7 of 12 subjects (58.3%).

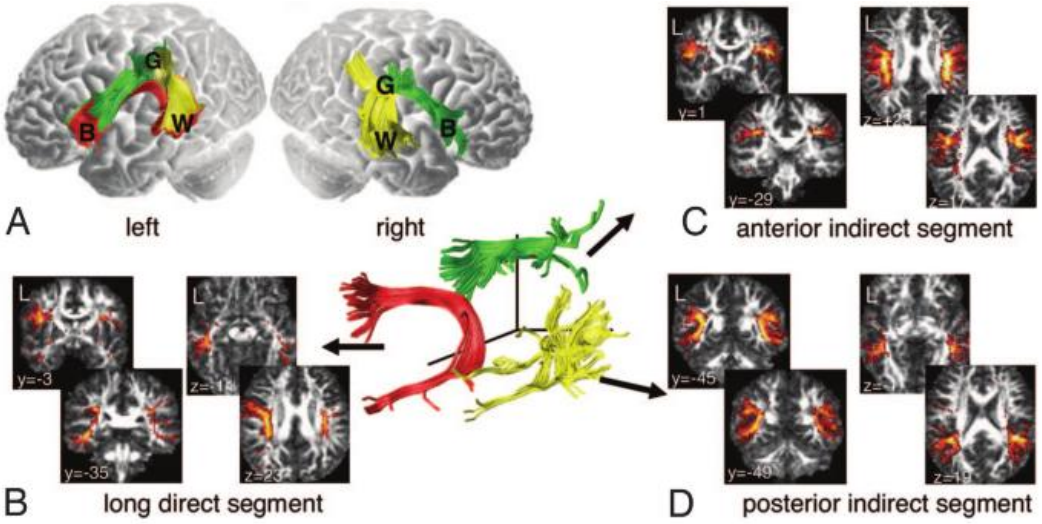

Figure 4. Superior longitudinal fasciculus (SLF) tractography reconstruction (A) of language pathways. The red long direct segment (arcuate fasciculus [AF]) connects Wernicke's and Broca's (B) areas only in the left hemisphere, and is medial to the indirect segments; bilaterally the posterior indirect yellow segment connects Wernick's area [superior posterior temporal cortex] and the inferior parietal lobe (Geschwind's territory); bilaterally the green anterior indirect segment connects the inferior parietal lobe (Geschwind's territory) with Broca's area in the inferior frontal cortex. B-D dissections of single brains (overlap maps) show leftward asymmetry only in the direct segment (AF). Reprinted from Catani et al. (2007).

However, in support of the Catani et al. (2005; 2007) findings and the more conventional AF configuration, recent probabilistic tractography has traced the AF through crossing fiber regions (AF and corticobulbar) to link Wernicke's and Broca's area seed points (Li et al., 2013). It warrants underlining, that probabilistic tractography was found more effective than deterministic tractography in tracing the entirety of the AF pathway (Li et al., 2013). Coursing parallel to the arcuate but ostensibly still part of the SLP is a dual segmented indirect pathway: the posterior portion connects the Wernicke's area to the inferior parietal lobe (Geschwind's territory) and the anterior segment connects the inferior parietal lobe with Broca's area (Catani, Jones & Dominic, 2005).

1.3 FA analyses of tract asymmetry

Of the main tracts, the AF (Buchel et al., 2004; Powell et al., 2006; Catani et al., 2007; Choi et al., 2010; Lebel and Beaulieu, 2009; O'Donnell et al., 2009; Oechslin et al., 2010; Upadhyay et al., 2008; Rodrigo et al., 2007; Takao, Hayashi, & Ohotomo, 2011) and cingulum (Gong et al., 2005; Kubicki et al., 2003; Park et al., 2004; Wang et al., 2004; Wakana et al., 2007; de Groot et al., 2009; Takao et al., 2011) are the most consistently reported tracts with leftward FA asymmetry. Buchel et al. (2004) found leftward FA asymmetry of AF in a group of healthy right-handed subjects ($p < 0.05$; n=15; age range 23-43; 4 females) as well as in a second group comprised of both healthy left-handed and right-handed ($p < 0.05$; n=28; age range 21-40; 9 left-handed, 19 right-handed; 14 females) subjects. Overall, the highest FA values were found in the left hemisphere AF and in the right hemisphere inferior parietal cortex. Powell et al. (2006) (n=10; age range 23-50; right-handed) reported greater overall leftward and AF FA ($p < 0.05$). Oechslin et al. (2010) reported leftward FA of the AF in perfect pitch-discerning musicians ($p <0.016$), while musicians without perfect pitch were bilaterally symmetric (n = 26, mean age 24.6 ± 3.3; 13 HCs). Catani et al. (2007) found leftward FA asymmetry of the AF (p = 0.035; n= 40 healthy right-handed subjects; 20 male, 20 female; age range 18-22). Choi et al. (2010) found AF leftward asymmetry in males and females collectively (p <0.001; n=43; mean age 25.5 ± 3.69; healthy right-handed; 21 females) as well as in female (p= 0.019) and male groups independently (p=0.008). In a large study

(*n*=183; age range 5-30, mean age 16.3 ± 6.8; healthy, right-handed; 86 females) Lebel and Beaulieu (2009) reported leftward FA asymmetry of the AF in children, adolescents and young adults ($p < 0.001$). In addition, the number of AF streamlines left lateralized approximated 84% (153/183; laterality index > 0); in 30 subjects streamlines were right lateralized. Lateralization was unaffected by age or gender. O' Donnell reported FA leftward asymmetry of the AF ($p < 0.005$; *n*=35; right-handed) that was associated with the lowest λ3 (smallest eigenvalue) value but highest λ1 (largest eigenvalue) value. Another much smaller study (*n*=4; mean age 32.25 ± 8.5; healthy, right-handed males) from Upadhyay et al. (2008) reported the use of diffusion spectroscopy of N-acetyl aspartate to reveal leftward FA asymmetry of the AF ($p <0.002$) not evidenced using the standard water-based diffusion tensor analysis. Rodrigo et al. (2007) reported AF leftward FA asymmetry ($p < .001$; *n*=18, 5 males, 13 females; mean age 24 ± 3.3; healthy, right-handed), with the uncinate and inferior occipital fasciculi contributing to the left lateralized AF asymmetry. Perlaki et al. (2013) in a study restricted to only left handed subjects (*n*= 16, 16 female; mean age 21 ± 1.7), reported that greater FA in the in left angular gyrus, left superior parietal lobe, and left SLF was associated with left hemisphere language lateralization, while reduced FA was associated with atypical language lateralization, the latter included language lateralization in the right precentral and inferior right frontal gyri ($p < 0.05$). Takao et al. (2011), in a study with a very large number of healthy subjects (*n*=857; age range 24.9-84.8; 310 females; handedness not disclosed), reported leftward FA asymmetry of the AF (range: $p < .025 – p < .0001$). The collective white matter FA asymmetry of all tracts was 39.9% rightward (22, 118 voxels) and 33% leftward (18,300 voxels).

De Groot et al. (2009), in a study with a large number of right-handed subjects (*n*=500; mean age 54.9 ± 5.52; 260 females), found greater leftward asymmetry of the anterior cingulum but greater rightward FA asymmetry in the posterior cingulum (*p*- value range < .05 - < .001). Kubicki et al.(2003), reported that right-handed schizophrenic patients had reduced bilateral FA compared to healthy controls (*n*= 16 schizophrenics; *n*=16 controls; age range 18-55). Park et al. (2004) found leftward FA asymmetry of the cingulum bundle in right-handed schizophrenia patients as well as right-handed healthy controls (HCs), though the leftward asymmetry was less pronounced in schizophrenia patients (age range: HCs 30-

55 ± 6.2; patients 28-53 ± 7.2; $p < .005$). Wakana et al. (2007) reported leftward asymmetry of the upper cingulum in 10 healthy subjects (5 female; mean age 26.1± 5.48; $p < .05$), and the Takao et al. (2011) study, referred to above (n= 857; age range 24.9 – 84.8; 310 females; handedness not reported) , reported leftward asymmetry of the anterior cingulum (range: $p < .025$ – $p < .0001$).

AF rightward FA asymmetry has been reported (Oechslin et al., 2010; Park et al., 2004), though less frequently than rightward asymmetry of the anterior indirect SLF segment and other main tracts (Catani et al., 2007; Hasan et al., 2010; Thiebaut de Schotten et al., 2011). In 32 right-handed HCs (age range 30-55 ± 6.2), Park et al. (2004) found rightward asymmetry of the AF (reported as including both the long direct SLF segment and the inferior longitudinal fasciculus [IL]), the anterior limb of the internal capsule (ALIC; [includes the anterior thalamic radiations and frontopontine fibers]), internal capsule and uncinate fasciculus (UN) ($p < 0.005$). In the same study, a similar pattern was reported for schizophrenic patients (n = 23; age range 28-53 ± 7.2). Oechslin et al. (2010), in a study involving musicians, reported rightward FA of the AF in HCs (p = 0.016; n = 26, mean age 24.6 ± 3.3; 13 HCs).

Rightward asymmetry of the anterior indirect segment of the SLF has also been reported with some frequency. Catani et al. (2007) found rightward asymmetry of the anterior indirect SLF (p = 0.001; n= 40 healthy right-handed subjects; 20 male, 20 female; age range 18-22), a segment previously mapped and defined the by Catani et al. (2005). Additionally of note in this study was the finding that those with bilaterally symmetrical language networks achieve higher performance in words learned through semantic association. Hasan et al. (2010) reported rightward FA asymmetry of the frontoparietal and frontotemporal AF segments (which seem to correspond to the SLF indirect segments [Catani et al., 2005] or SLF-I [Makris et al., 2005]) for 77 right-handed healthy adults ($p < 0.0001$; 45 females, mean age 38 ± 13.5; 32 males, mean age 36.7 ± 13.5) as well as rightward FA asymmetry of just the frontoparietal AF in 42 right-handed healthy children and adolescents ($p < 0.0001$; 20 females, mean age 10.3 ± 2.9; 22 males, mean age 11.7 ± 3.2) . Thiebaut di Schotten et al. (2010), in a study involving 40 young healthy adults (n= 20 males, n=20 females; age range 18-22) reported rightward FA asymmetry of the SLF anterior indirect segment ($p < 0.001$) and optic radiation ($p < 0.001$) as well as overall leftward AF (tractography)

streamline asymmetry but rightward streamline asymmetry of the indirect anterior SLF and inferior fronto-occipital fasciculus, findings generally consistent with those of Catani et al. (2007).

1.4 Training-associated brain structure alterations

Most germane to the current study, and as noted at the outset, FA asymmetry and WM/GM volumetric asymmetries and alterations are associated with training and expertise (Bengtsson et al., 2005; Boyke, Driemeyer, Gaser, Buchel, & May, 2008; Colcombe et al., 2006; Draganski et al., 2004; Driemeyer, Boyke, Gaser, Buchel, & May, 2008; Halwani, Loui, Ruber, & Schlaug, 2011; Hanggi, Koeneke, Bezzola, & Jancke, 2010; Imfeld, Oechslin, Meyer, Loenneker & Jancke, 2009; Ilg et al., 2008; Koeneke, Hoppe, Rominger, & Hanggi, 2009; Nigmatullina, Hellyer, Nachev, Sharp, & Seemungal, 2013; Schmithorst & Wilke, 2002; Scholz, Klein, Behrens, & Johensen-Berg, 2009, Wang et al., 2012). Investigation of brain structure FA and volumetric alterations has been conducted for newly acquired skills (e.g. meditation and juggling) and expert groups with long-term training, including dancers, musicians, elite gymnasts, and golfers. Structural alterations in expert and newly trained groups might be divided into training-associated increases (Bengtsson et al., 2005; Boyke et al., 2008; Draganski et al., 2004; Halwani et al., 2011; Hufner et al. 2011; Ilg, et al., 2008; Janeke et al. 2009; Keller & Just, 2009; Maguire et al., 2000; Scholz et al., 2009; Schmithorst & Wilke, 2002; Takeuchi et al., 2010, Taubert et al., 2010; Wang et al., 2012) and training-associated decreases (Hanggi et al., 2010; Imfeld et al., 2009; Nigmatullina et al., 2013), but this is a specious distinction; most of studies referenced in this paragraph reported both training-associated structural increases and decreases underlining that structural change is generally not a uniform process across the brain.

Keller and Just (2009) reported that 100 hours of intensive remedial reading for right-handed 8-10 year old children (n= 35; HCs 12) resulted in a shift from low FA in a segment of the left anterior centrum semiovale to athletically high FA in the same region ($p < 0.05$); a change correlated with decreased RD. Relative to HCs, Scholz et al. (2009) found increased FA in WM of the right posterior parietal sulcus ($p < 0.05$) in newly trained jugglers with 6 months of juggling practice (n = 48, 24 trained; 24 HCs).

Takeuchi et al. (2010) reported 2 months of daily working memory training (25 minute sessions) for eleven right handed participants (n = 11, 3 females; mean age 21.2 ± 1.44) increased FA ($p < 0.05$) in the anterior corpus callosum ($p < 0.05$) and the right inferior parietal sulcus ($p < 0.001$). In musicians with continuous childhood-to-adult training, Bengtsson et al. (2005) reported higher FA in right posterior limb of the internal capsule relative to HCs ($p < .0001$; n = 16; 8 right-handed, musicians, mean age= 32.6, ± 5.7; 8 HCs; 8 males).The former study also reported a significant correlation between childhood practice and FA but no correlation between FA and adolescent or adult practice. Musicians have shown reduced bilateral FA of the internal capsule (p = 0.005), but increased bilateral FA in the genu of the corpus callosum (p = 0.003) (n = 11; 5 musicians, mean age=31.2 ± 11.2; 6 HCs) (Schmithorst & Wilke, 2002). A study by Oechslin et al. (2010) of right handed participants, noted previously, reported leftward FA of the AF in perfect pitch-discerning (PPD) musicians (p <0.016) while musicians without perfect pitch were bilaterally symmetric (n = 26, 13 PPD musicians, mean age 24.6 ± 3.3; 13 musicians with relative pitch perception), and HCs had rightward FA of the AF (p = 0.016; n = 13, mean age 25.6 ± 5.3). Steele (2012) reported right-handed musicians (n=13; age range 18-27, mean age 22.4 ± 2.9; 5 females) FA was negatively correlated with performance on a motor learning task ($p > 0.05$) and interpreted the finding as mediated by a positive correlation with radial diffusivity ($p < 0.005$) localized to crossing fibers of the SLF and corticospinal tracts (CST) bilaterally in the somatosensory cortex. Imfeld et al. (2009) reported reduced FA ($p < 0.05$) bilaterally in the CST of right-hand musicians (n=26; mean age 24.6 ± 2.9; 16 females) compared to controls (n=13; mean 25.6 ± 5.3; 7 females). Wang et al. (2012) reported greater FA in both the left (p=0.012) and right (p= 0.011) CST of right-handed, world class gymnasts (n=13; mean age 20.5 ± 3.2; 7 females) relative to HCs (n= 14; mean age 22.3 ± 2.7; 7 females); reduced RD values were also found bilaterally in the CST of the gymnasts. In a study involving both vocal and instrumental musicians (n=22 musicians: 11 vocalists [8 female], 11 instrumentalists [6 female]; 11 HCs, mean age 26.8 ± 1.33), Halwani et al. (2011), reported greater bilateral FA of the AF in both musician groups relative to HCs ($p < 0.001$). Also, instrumentalists had higher FA (but lower tract volume) compared to vocalists in the left dorsal region of the AF (p = 0.002).

Maguire et al., (2000) elevated the profile of cab drivers with the finding that the bilateral posterior hippocampi of right handed taxi drivers had greater volume relative to HCs ($p < 0.05$), a volume metric that was positively correlated with time as a cab driver. Conversely, the anterior hippocampi in HCs showed greater volume relative to the anterior hippocampi of taxi drivers (n= 66, 16 cab drivers, mean age 44, 0 female; 50 HCs, 0 female; mean age 44). A study by Draganski et al. (2004) was one of the first to demonstrate GM training-induced changes in the adult brain in response to juggling training (n= 24; 12 trained; 12 HCs; mean age 22 ± 1.6; 21 female), using young adults with no prior juggling experience. After a 3 month training period, the juggler group showed a peak bilateral GM increase relative to HCs in the motion sensitive occipito-temporal (hMT/V5) area ($p < 0.05$), a difference that diminished by the end of a subsequent non-training 3 month interval. In another follow-up study from the same research camp (Arne May), Boyke et al., (2008) found a similar though less pronounced transient increase in GM associated with learning to juggle in 69 senior citizens (n = 44, 24 female; mean age 59.1; 25 HCs, 17 female, mean age 60.2), but lateralized to the right hemisphere hMT/V5 area ($p < 0.05$). In professional ballet dancers (n = 20, 10 dancers, mean age 21.3 ± 3, 10 females; 10 HCs), and compared to healthy controls, Hanggi et al. (2010) reported reduced FA ($p < 0.01$) in WM underlying the bilateral premotor cortex , right frontal operculum and left middle frontal gyrus. FA was not correlated with years of dance training. Years of training, however, was negatively correlated with GM volume in the right premotor cortex and WM volume in the bilateral internal capsule, but positively correlated with WM volume in the CC and left precentral gyrus. There were multiple WM and GM reductions in dancers relative to HCs, with WM reductions of the left anterior cingulum, bilateral corticospinal tract, corpus callosum, and the bilateral internal capsules; and GM reductions of superior frontal gyrus (SFG), putamen, the left supplementary motor area (SMA), and left premotor cortex. Janeke et al. (2009) examined structural parameters in a combined group of professional and non-professional but skilled golfers relative to a combined group of less skilled golfers and non-golfers (n = 40; 10 professional golfers, mean age 30 ± 6.2; 10 skilled golfers, mean age 26.6 ± 8.3; 10 less skilled golfers, mean age 26.5 ± 3.4; 10 non-golfers, mean age 25.9 ± 2; 0 female; 80% right handed). Findings included higher GM

volume in the right dorsal premotor cortex (p =0.012), left posterior dorsal premotor cortex (p = 0.029), left posterior intraparietal sulcus (p = 0.013) and the medial posterior parietal cortex (0.019), for the professional/skilled group but reduced WM volume for this group (p <0.05) in the cortical spinal tract and parietal operculum. In addition, reduced FA was reported for the professional/skilled group in areas including the internal capsule, coronal radiata and posterior aspect of the corpus callosum (p < .10). In a study involving 59 older (range 65 - 70) sedentary adults (32 female) split into two groups, Colcombe et al. (2006) reported increased GM (p < 0.05) and WM (p < 0.05) volumes for the group that engaged in 6-months of aerobic training relative to age-matched non-aerobically trained controls. The GM and WM volume increases for the trained group were primarily located in the temporal and prefrontal cortices. Ilg et al. (2008) reported that 2 weeks of practice in a mirror reading task increased GM volume (p < 0 .05) in the right occipital cortex within the practice group relative to HCs (n= 38; 20 trained; 18 HCs; age range 20 – 32; right handed). A study by Nigmatullina et al. (2013) involving professional ballet dancers (n = 49; 29 dancers, mean age 21.9 ± 3.2; mean years of dance experience 16; 20 HCs) reported GM volume in the posterior bilateral vestibular cerebellum (p < 0.05) was negatively correlated with years of dance experience; dancers demonstrated reduced GM volume relative to controls. It was posited as related to attenuated vertigo response in dancers relative to HCs. Interestingly, the same study reported increased dancer GM volume in the superior aspect of the right superior orbitofrontal cortex. A study by Taubert, et al. (2010), involving an entire-body balance (n = 28; 14 trained; 14 HCs; 14 female; mean age 25.9 ± 2.8; 28, right-handed) reported GM increase (p <0.05), relative to HCs, in the left superior orbitofrontal cortex, left superior frontal gyrus (SFG), and left supplementary motor area of subjects newly trained in a whole-body balance task who underwent 6 weeks duration of training. Antithetically, training was associated with a GM volume decrease in the right inferior orbitofrontal cortex and other right-side structures as well as the left cerebellum (p <0.05). FA was reported as reduced in the bilateral WM of the prefrontal regions (p <0.05) in proximity of the GM alterations, a finding posited to be a training related recruitment of crossing fibers. Taubert, et al. (2010) also reported that GM increase in the prefrontal cortex was positively correlated with balance skill performance improvement (p <0.05). Hufner et al.

(2010) used 7 professional ballet dancers, 7 slackliners, and 7 ice dancers, which collectively constituted the trained group, as well as 20 HCs (n = 21; 11 female, mean age 24.9 ± 7.82; 20 HCs, 12 female, mean age 26.65 ± 4.96) in a learning and memory study. The findings were similar to those reported by Maguire et al. (2000). In the trained group relative to HCs there was greater GM volume bilaterally in posterior hippocampal and parahippocampal ROIs ($p < 0.05$), but by contrast, HCs demonstrated greater volume of GM in bilateral anterior hippocampal/parahippocampal regions and in the bilateral insular cortex ROIs ($p <0.05$).

1.5 Objectives

To the best of our knowledge, none of the studies reviewed in the introduction, or published but not reviewed here, assessed whole brain FA lateralization differences (left-minus-right [L-R] bilateral differences in homologous structures) in dancers relative to HCs. It was hypothesized that between-group FA lateralization would differ between dancers and HCs. Based on the literature review, it was further hypothesized that there would be greater dancer FA compared to HCs localized to specific structures. In short, both differing FA asymmetry and absolute FA differences were expected between groups. It was also predicted that while between group differences would occur, there would be similar overall patterns of leftward and rightward FA lateralization. Finally, it was posited that global WM/GM volumes would differ between groups.

Chapter Two

Method

2.1 Subjects

This study included 18 right handed subjects: *n* = 9 male, professional ballet dancers:, age range 18-50, mean age 23 ± 10.21; 9 HCs, 4 female, age range 23 – 27, mean age 24.89 ± 1.70. Dancer years of experience ranged from 7-44 years (mean 13.83 ± 11.71). The York University Human Participants Review Subcommittee approved the magnetic resonance imaging (MR) required in this research, and participants were interviewed and gave informed consent prior to the study.

2.2 Imaging data acquisition

T1 structural, and diffusion tensor images (DTI) were acquired with a Siemens 3T Magnetom Trio Tim MRI (Siemens Medical Solutions, Erlangen, Germany) scanner equipped with a 32-channel head coil. T1 specifications included a fast spin echo protocol, coronal 1.0 mm slices, TR= 1900 ms, TE = 252 ms, matrix resolution of 256 x 256, field of view (FOV) read 256 mm, FOV phase 100% , flip angle 90°. In respect to diffusion-weighted data, there were 30 directions with b-values of 1000 s/mm2 along which diffusion weighting was applied; there was a single volume with no diffusion weighting (b-value= 0 [b_0]). Diffusion tenor images were acquired using spin-echo echo planar sequence in 60 slices, TR= 8300 ms, TE= 100 ms, FOV= 240 mm, slice thickness= 2.0 mm, echo spacing= .74 ms, image matrix = 240 x 240 x 120.

2.3 Imaging analysis

Brain extraction of T1 images was conducted with FSL's brain extraction tool (BET; Smith 2002). Global WM and GM volume analyses were conducted using FSL FAST (Zhang, Brady, & Smith, 2001). Image processing was of diffusion tensor images was conducted with FSL TBSS, part of FMRIB's Software Library 5.0.1, http://www.fmrib.ox.ac.uk/fsl) (Smith et al., 2004). Initially, the raw data was head-motion and eddy current corrected using FMRIB's Diffusion Toolbox (FDT) (Smith et al., 2004). This was followed by brain extraction using BET (Smith, 2002) and the creation of a no diffusion-

weighted mask. FA tensors were then fitted to the diffusion-weighted data (DWI) using DTIFIT, part of FDT. FA data from all subjects was subsequently copied and placed in a folder for tract-based spatial statistics (TBSS) analysis (Smith et al., 2006). Brain diffusion parameter analyses (FA, AD, MD, RD) were preceded by alignment of all participants FA data (4D image) to a standardized Montreal Neurological Institute (MNI) 152 space using non-linear registration, part of FMRIB's Software Library 5.0.1, http://www.fmrib.ox.ac.uk/fsl) (Smith et al., 2004). Following standard TBSS procedures, a mean "skeletonized" FA image was created, an image representative of common tract centers across participants; individual participants aligned FA data was then projected onto the skeletonized mean FA image. The use of a mean FA skeleton reduces extremes by providing an FA core and makes the distribution more Gaussian (though normality is not a factor in TBSS analysis given the permutation statistical approach adopted does not require a normal distribution). Subsequently, a "tbss_sym" script was used to create yet another mean FA image, but one with general correspondence between left and right tract structure. The aligned FA 4D image from all participants is then projected onto a symmetrized skeleton resulting in an all FA symmetrized skeleton image (again this is a mean image of tracts common to the group). For details regarding TBSS procedures, see Smith et al. (2006) and the TBSS user guide (http://fsl.fmrib.ox.ac.uk/fsl/fslwiki/TBSS/UserGuide). Finally, this skeletonized image was left-right flipped and subtracted from the original 4D image, (such that the right side of standard space corresponded to the left half of the dataset), and the left side was zeroed given that the same information was now present on both sides.

Procedurally, and as mentioned at the end of the introduction, first left vs right hemisphere regional FA asymmetry was evaluated for dancers and HCs separately with 1-sample imaging analyses using the tbss_sym FA script (Smith et al., 2006); global FA 1-sample tests were then conducted (dancers and HCs separately). Subsequently, global WM and GM volumes were assessed between-groups. Finally, two between group FA analyses were conducted: the tbss_sym script was used to localize FA lateralization differences and the TBSS script (Smith et al., 2006) was used to localize absolute FA differences. It should be understood that the 1-sample tbyss_sym FA script tests where, in which tract or

tract aspect, L-R significantly differs from zero; no difference between left and right occurs if L-R does not significantly differ from zero. The 1-sample tbss_sym FA script and the global 1-sample FA tests can be interpreted as absolute indicators of L>R FA or R>L FA (they actually test if L-R difference > 0). Similarly the TBSS between-group FA analysis will calculate the areas of greater or reduced FA between groups. However, the tbss_sym between-group analysis tests bilateral differences (L-R) in structures, as opposed to absolute differences. In respect to covariates, age was included as a covariate for dancers while both age and sex were included as covariates for HCs. Age and sex were demeaned prior to inclusion as covariates.

2.4 Statistical analysis

The dependent variable was FA and the independent predictor variable was training. Exploratory (α= 0.10) and standard (α= 0.05) thresholds were applied to DTI (e.g. FA) image maps for both the lateralization and absolute FA image analyses; each threshold map was FWE corrected. Including a less stringent statistical threshold was deemed appropriate given the novel, exploratory nature of the project (in respect to the FA asymmetry analysis) and the small number of study subjects. The standard level of significance of α= 0.05 was used for macrostructural volumetric analyses because although the number of study subjects was small such analyses are quite routine in training related research (see introduction). All correlational analyses where thresholded at α =0.05.

To localize FA asymmetry, 1-sample and between sample FA analyses were conducted using tbss_sym FA script. The 1-sample analyses tested if left-minus-right (L-R) and right-minus-left (R-L) FA significantly differed from zero and was positive in dancers and control groups separately. The images were thresholded only at α= 0.10 because the objective here was to assess gross patterns: L>R or R>L in each group. FA asymmetry in the 1-sample and between-groups tests were statistically evaluated using the voxel-wise permutation strategy of Nichols and Holmes (2002) as implemented in the FSL randomize tool (this results in one t-statistic for each voxel, not an overall t-value). The latter is a non-parametric permutation approach controlling for family-wise multiple comparison error. Nevertheless, the false discovery rate (FDR) method of multiple comparison correction was also used. If FDR p-values were

higher (less significant) than permutation-derived p-values, the FDR p-values were used. Each group (dancers and HCs) was analyzed separately using a tbss_sym FA analysis and a global FA analysis. This was followed by between group comparisons using tbss_sym FA (Smith et al., 2006), TBSS (Smith et al., 2006) and FAST (Zhang, Brady, & Smith 2001). The 1-sample (tbyss_sym FA) dancer FA analysis localizing main tract asymmetry controlled for age and used three t-contrasts for both left FA greater than zero then for right FA greater than zero (e.g. L>0, positive effect of age, negative effect of age). The HCs 1-sample (tbyss_sym FA) analysis controlled for age and gender, and used four t-contrasts (e.g. L>0, positive effect of age, negative effect of age, effect of gender). There were 512 permutations for each contrast in the 1-sample analyses.

Controlling for age and gender (covariates of no interest), there were 5000 permutations for the between groups tbss_sym and TBSS analyses; the latter had five t-contrasts (HCs - dancers: [1 -1]; dancers - HCs [-1 1], positive effect of age, negative effect of age, effect of gender). For both group and between group tbyss_sym FA and TBSS analyses, clusters of significant voxels (FWE corrected) were generated and displayed on the FA-skeleton, effect size maps were created (Cohen's *d*), and cluster reports were created. Visual inspection of the JHU White-Matter Tractography and Juelich Histological Atlases was used to associate cluster-report significant voxels (the raw t-statistic masked by the corrected p-values) with tracts to determine significant voxel tract assignment. Global 1-sample FA calculations (for dancer and HCs groups separately) were thresholded at the traditional $\alpha=0.05$ level of significance. Calculations were completed by creation of a region of interest mask for each hemisphere and summing left and right hemisphere FA separately. In addition, a between-group comparison of global WM and GM volume was completed using FSL FAST (Zhang, Brady, & Smith, 2001); a significance level of $\alpha=0.05$ was used.

Potential correlations assessed across groups were FA and years of experience, FA and age, and FA and gender. Correlations were also assessed between FA and AD, FA and MD and FA and RD. The AD, MD and RD values were captured within a sphere mask centered at the between group difference

MNI max coordinates. Correlations between volume (WM and GM) and the variables age, sex years of experience across groups were also completed. Global histograms of the collective dancer and HCs pre-"skeletonized" and post "skeletonized " FA were computed, and the Kolmogorov-Smirnov normality test adapted by Lilliefors (1967) was used to assess histogram data relative normality: FA distribution is ostensibly made more Gaussian through the TBSS creation of mean FA skeleton. Statistical analyses extraneous to tbss_sym and TBSS permutation tests were conducted in *R* (R 3.0.1, R Development Core Team, 2013).

Chapter Three

Results

The histogram assessment of global FA distribution relative normality will be reported first. This will be followed by review of the global FA and tbss_sym FA analyses for each group. Subsequently, the between group volumetric and between group FA results from both the tbss_sym and TBSS analyses will be reported. The Global histogram derived from the skeletonized FA mean image of dancers and HCs showed relatively normal distribution shape based on a Lilliefors (1967) analysis. This can be seen in the bottom row of Figure 5 which shows the FA (mean) skeleton on the left and the post skeletonized p-value distribution on the right; the latter is largely in the normal range. By contrast, the pre-skeletonized all FA histogram in the top row of Figure 5 is positively skewed and the p-values of this distribution, on the right, are largely non-normal. This demonstrated that the TBSS mean FA skeleton did produce a relatively normal FA distribution, ostensibly guaranteeing sufficient normality for accuracy of standard t-tests (Welch) used for the global FA and volumetric analyses, which did not use the permutation analysis employed in the tbss_sym FA and TBSS analyses. Additional indices of relative distribution normality were also used prior to the global FA volumetric tests (see below).

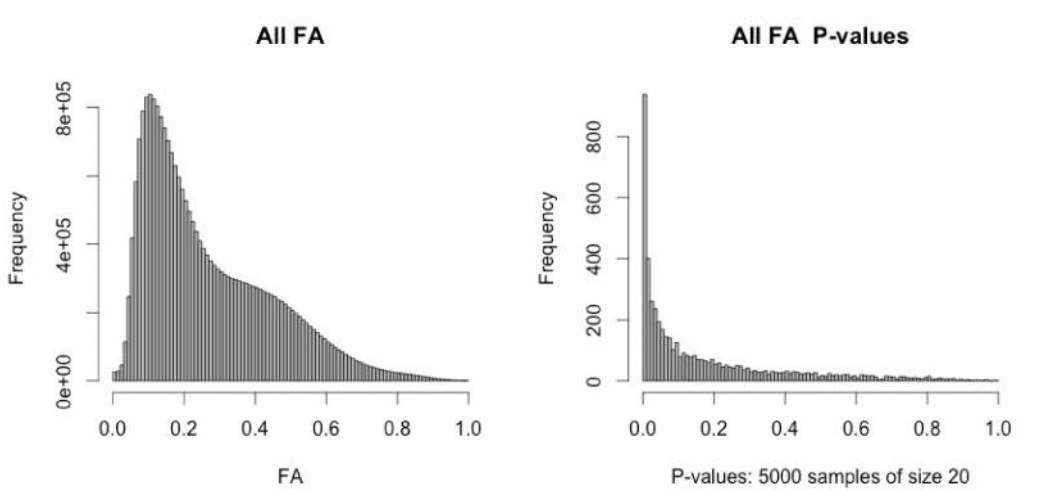

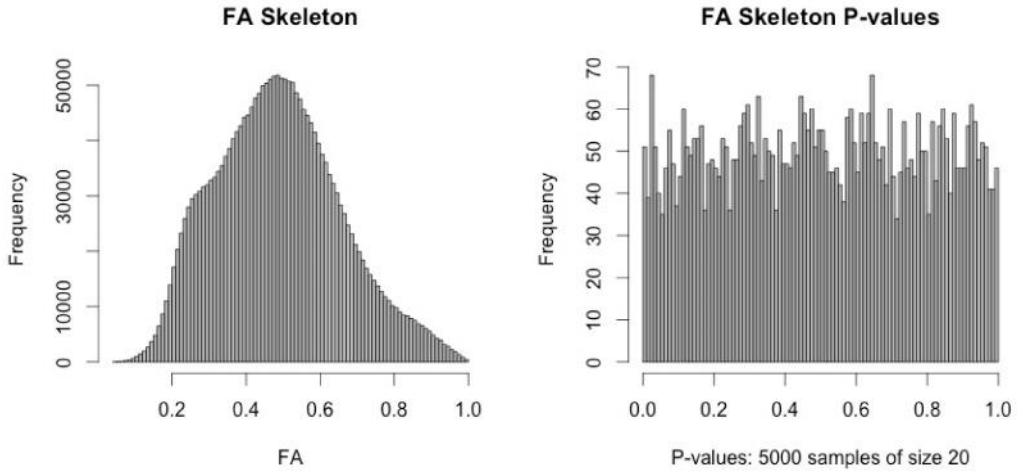

Figure 5. Top row, left: histogram of all subjects global (All FA); right: histogram of p-values (All FA) based on Lilliefors (1967). Note, ~ 60% of the p-values are in the non-normal range. Bottom row, left: histogram of the All FA skeleton; right: histogram of p-values (All FA skeleton) based on Lilliefors (1967). Note, ~ 95% of the p-values are in the normal range. HCs=healthy controls; FA=fractional anisotropy

For both dancer and HCs groups, FA distribution normality (e.g. Shapiro-Wilk) and homogeneity of variance (Levene's Test) tests were conducted prior to running 1-sample t-tests on the global FA difference (L-R) between hemispheres, and there were no significant violations of normality. For dancers, the mean global left hemisphere FA (M = 0.5006 ± 0.0252) and mean global right hemisphere FA (M= 0.4664 ± 0.022) differed, with the left showing higher FA. A 1-sample L-R FA t-test (Welch) revealed that L-R significantly differed from zero, $t(8) = 18.89$, $p < .0001$, d= 6.30, indicating that left and right FA significantly differed (if there was no difference between left and right then L-R would not have significantly differed from zero), supporting greater leftward FA lateralization. The results for HCs were very similar: mean global left hemisphere FA (M = 0.4996 ± 0.0168) and mean global right hemisphere FA (M= 0.4651 ± 0.0163) differed, with the left also showing higher FA. A 1-sample L-R FA analysis t-test revealed that L-R significantly differed from zero, $t(8)$= 22.50, $p < .0001$, d = 7.5 indicating that left

and right FA significantly differed, supporting higher leftward FA. The box plots in Figure 6 characterize the left hemisphere vs right hemisphere global FA difference for dancers (left box plot) and HCs (right box plot) respectively. The non-overlapping notches in the boxplots indicate a high probability that FA between hemispheres differs (McGill, Tukey & Larsen, 1978). Note, the outliers evident in the data were removed with a 20% symmetric trimmed mean removing the 2 top and 2 lowest scores. This resulted in the same pattern of L-R >0, with left FA thus differing from right FA, $t(4)=25.56$, $p<0.0001$, $d = 11.43$. In short, for both groups, the global L-R FA difference significantly differed from zero and was positive, and there was definitive leftward FA asymmetry in dancers and HCs. However, there was no significant difference in global FA asymmetry between groups, $t(15.58)=0.15$, $p=.88$, $r^2=.001$.

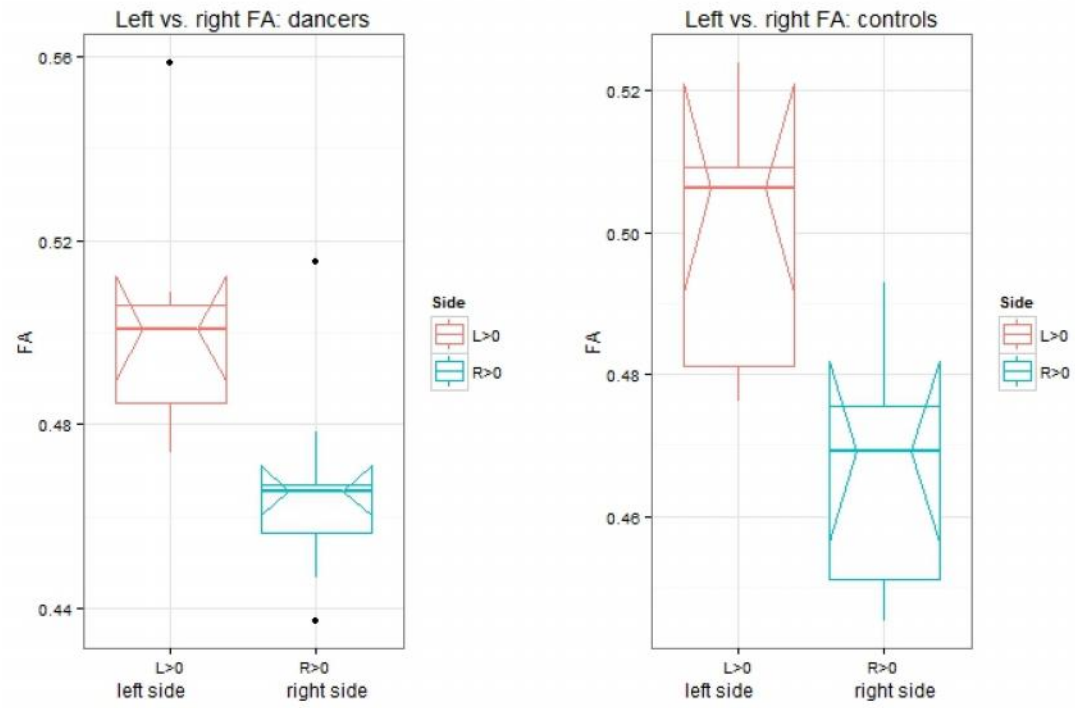

Figure 6. Left: boxplot of dancer global FA asymmetry, L-R and R-L: most values are in the upper extent of the 50% interquartile range; right: boxplot of HCs' global FA L-R and R-L asymmetry. The non-overlapping notches in the boxplots indicate a high probability that FA between hemispheres differs (McGill, Tukey & Larsen, 1978). HCs=healthy controls; FA=fractional anisotropy.

Prior to reporting imaging analyses results (tbss_sym and TBSS scripts), it should be mentioned that the images in this study used Cohen's *d* to measure effect size. Although the range of Cohen's *d* is .2 to .8 for all images, for visualization purposes the upper end of the range was set in FSLview (www.fmrib.xo.ac.uk/fsl/fslview) to 1.95 to improve visual contrast of areas 2 to 3 standard deviations above the mean. It is underlined that this merely facilitated the visual distinctiveness of differing effect sizes across relevant areas and in no way altered the actual value of the Cohen's *d* statistic. Also, as mentioned previously, to identify structures associated with significantly different FA in the tbss_sym and TBSS analyses images the JHU White-Matter Tractography, and Juelich Histological Atlases integrated with FSLView v3.1 (FMRIB Software Library) were used. The Harvard-Oxford Cortical Atlas was also used to identify relevant GM structures. Structure probabilistic identities were derived from reference to the above referenced Atlases.

Tbss_sym (1-sample) FA analyses for each group located in which tract or tract aspect left-minus-right and right-minus-left FA values significantly differed from zero (L-R>0; R-L>0) and were positive (α= 0.10). This test is therefore very similar to the global FA test except that it localizes structure FA asymmetry. The dancer mean L-R FA (M = 0.0973 ± 0.0144) was higher than dancer mean R-L FA (M = 0.0701 ± 0.0086), significantly differed from zero, $p < 0.10$ (FWE corrected), was positive, and there was definitive leftward FA asymmetry. Table 1 of Appendix A lists the numerous structures of L>R FA in dancers and their MNI max coordinates. Similarly, the mean L-R FA of the HCs (M = 0.0852 ± 0.016) was higher than the HCs' R-L mean FA (M = 0.0595 ± 0.0098), significantly differed from zero, $p < 0.10$ (FWE corrected), was positive, and there was definitive leftward FA asymmetry. Table 2 of Appendix A lists the numerous structures for HCs' L>R FA and the MNI max coordinates of these structures. The effects of age and gender on FA were not significant for dancers or HCs. The 1-sample tbss_sym FA test can be viewed as evaluating absolute asymmetry of L>R or R>L, reflecting that a voxel can not be most lateralized to the left and right hemispheres at the same time. The bar graphs in Figure 7 characterize the L>R and R>L FA asymmetries in dancers (left bar graph) and HCs (right bar graph). The

non-overlapping 95% CI error bars in Figure 8 (point range) indicate a significant difference (Payton, Greenstone, Schenker, 2003) between left and right hemisphere FA for both dancers and HCs.

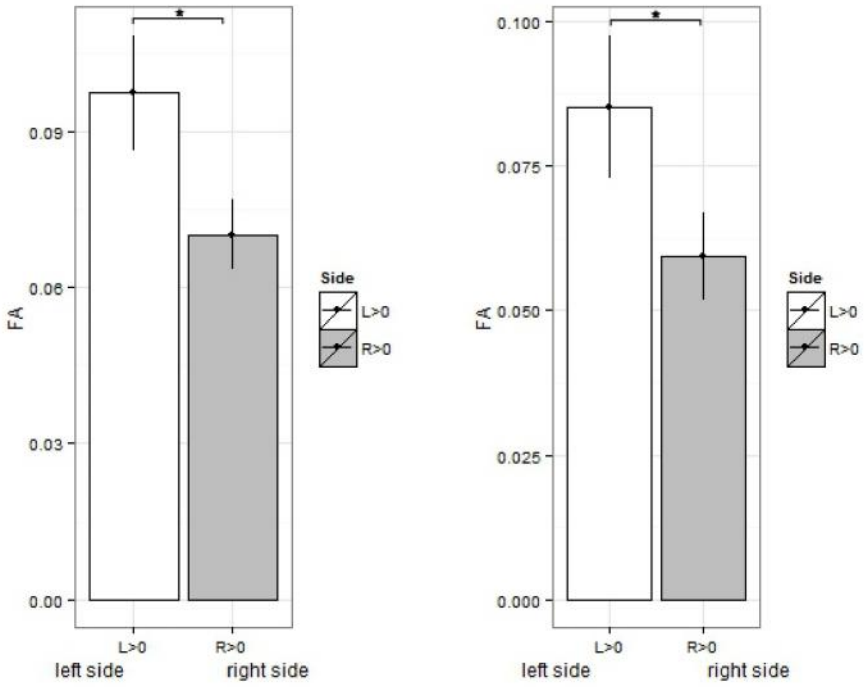

Figure 7. Left: L>R and R>L FA asymmetries for dancers; right: L>R and R>L FA HCs. Error bars represent the 95% confidence interval point range. The non-overlapping 95% CI error bars indicate a significant difference (Payton, Greenstone, Schenker, 2003) between left and right hemisphere FA for both dancers and HCs. FA=fractional anisotropy; L>R=left greater than right; R>L=right greater than left; HCs=healthy controls; * $p < 0.10$.

Prior to running a global WM and GM between-groups analysis, normality (e.g. Shapiro-Wilks) and homogeneity of variance (Levene Test) tests were conducted for the data set of dancer and HCs groups and there were no significant violations of normality. In addition, the WM volume variance ratio for HCs and dancers was 1.65, and the GM volume variance ratio was 1.54; both ratios indicate homogeneity of variance between the groups. Dancers had higher mean WM (units: 1 mm isotropic

voxels) volume (M = 670743.1 ± 55659.37) compared to HCs (M = 603352.0, ± 71597.19). This difference was significant, $t(15.083) = 2.23$, $p < .05$, $r^2 = .25$. The 25% variance shared by WM volume and dance training is a large effect. On average, dancers also had more GM (M = 769242.3 ± 75103.56) than HCs (M = 674142.6 ± 60552.75), a difference that proved to be significant, $t(15.311) = 2.96$, $p < .01$, $r^2 = .36$. The 36% variance shared by GM volume and dance training is also a large effect. Graphs in Figure 8 depict dancer vs. HCs WM (a), and GM (b) volumes. Age and gender were not significantly correlated with WM volume: age, $r_s = -.46$, $p = .06$, $r_s^2 = .22$; gender, $r_{pb} = .25$, $r^2_{pb} = .06$, $p = .31$. However, there was a strong, positive correlation between years of dance training experience and WM volume, $r_s = .55$, $p < .05$, $r_s^2 = .31$. For GM volume, significant correlations were found between both GM volume and years of experience, and GM volume and age: there was a strong positive correlation between years of training experience and GM volume, $r_s = .61$, $p < .01$, $r_s^2 = .38$; there was a strong negative correlation between age and GM, $r_s = -.69$, $p < .01$, $r_s^2 = .48$. Gender was not significantly correlated with GM volume, $r_{pb} = -.25$, $p = .31$, $r^2_{pb} = .06$.

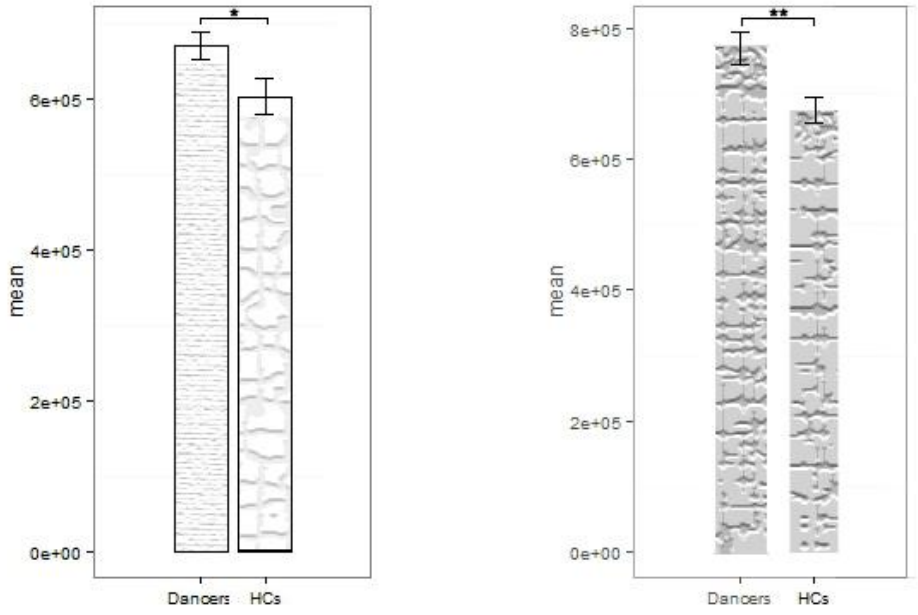

Figure 8. Left: WM volume of dancers was greater than HCs, * $p < 0.05$; right: GM volume of dancers was greater than HCs, ** $p < 0.01$. Error bars indicate the standard error of the mean. Y-axes show the mean number of 1mm voxels. WM= white matter; GM = grey matter; HCs= healthy controls

The L-R FA asymmetry analysis (tbss_sym FA) localizing bilateral FA differences between-groups revealed that dancers had higher L-R FA ($M = 0.055 \pm 0.0261$) relative to HCs ($M = -0.0329 \pm 0.0413$).This difference was significant, $p < 0.10$ (FWE corrected). Table 1 lists effect sizes (Cohen's d) of significantly different FA voxels and the underlying probable (probability expressed as a percentage) structures represented by these voxels. Effect sizes are high, indicating a large effect of lateralization, and specifically leftward FA asymmetry associated with dance training. This is characterized by the graph in Figure 9 (left) and the FA asymmetry images shown in Figure 10 (in the latter, both left and right FA is displayed in the left hemisphere). Because this is a bilateral difference between groups, HCs had higher R-L FA, greater rightward FA asymmetry ($Mdn = 0.0436 \pm 0.0408$) compared to dancers ($Mdn = -0.0519 \pm 0.0274$). This difference was also significant, $p < 0.10$ (FWE corrected). The rightward lateralization of HCs is depicted by the line graph on the right side of Figure 9. In Figure 9, the negative and positive FA values in the y-axis illustrate that this voxel-wise FA analysis exposes between-group FA asymmetry differences across the hemispheres. Bilateral between-group differences occur in a given structure; as such, FA values in the y-axis are not absolute (unlike the 1-sample analyses) and can be negative. The leftward FA of dancers relative to HCs is evident in the left line graph (L-R FA): dancers have positive FA values compared to HCs; a pattern that is reversed in the R-L FA analysis depicted in the right line graph, which shows the mainly positive values of HCs rightward FA relative to dancers negative rightward FA. Note, however that Figure 9 also shows that overall, the L-R FA values of dancers depicted in the left line graph are higher than the R-L FA values of HCs depicted in the right line graph. The leftward FA (L-R FA) asymmetry images shown in Figure 10 highlight peak output listed in Table 1 from the tbss_sym cluster report; images are displayed in the axial radiological convention. Illustrative of how this analysis exposes the bilateral FA difference of homologous structures, the cingulum and callosal

body had the greatest bilateral difference in FA asymmetry: highest leftward FA lateralization in dancers (Table 1), but highest rightward lateralization in HCs (Table 2). The largest cluster of significant voxels centered at the lowest p-value (p =0.052) was, as just mentioned, identified as including the posterior cingulum (11% probability) by reference to the JHU White-Matter Tractography Atlas, and the callosal body (10% probability) by reference to the Juelich Histological Atlas. This cluster was centered at MNI max coordinate -15 -56 28. Images in Figure 10 are arranged in ascending order from smallest p-value in the first row (greatest significance) to largest p-value in the last row. The MNI coordinate (-17 22 41) for which the JHU White-Matter Tractography Atlas found no tract label, is an exception in that it has a larger p-value than the subsequent max MNI coordinate. This coordinate and the associated (49 voxel) cluster was identified as the WM underlying the superior frontal gyrus (SFG) using the Harvard-Oxford Cortical Atlas (8% probability). This cluster was not identifiable as a specific tract perhaps because of crossing fibers. The cluster order in Figure 10 follows the order of clusters in Table 1. In addition, each image is associated with an effect size (Cohen's *d*) with a range of .2 to .8. To facilitate the visual differentiation of the range of effect sizes, the upper level of the effect size range was set to 1.95 (as noted previously, this is a visual aid only and does not alter the actual effect sizes). Note that larger, higher intensity clusters in the top row of Figure 10 persist and spatially expand through layers in the images of the lower rows where p-values are higher. An image of the last cluster of Table 1 is not shown (it consisted of just one voxel). Rightward FA asymmetry images (R-L) are not shown as they were essentially identical to the L-R leftward FA asymmetry images.

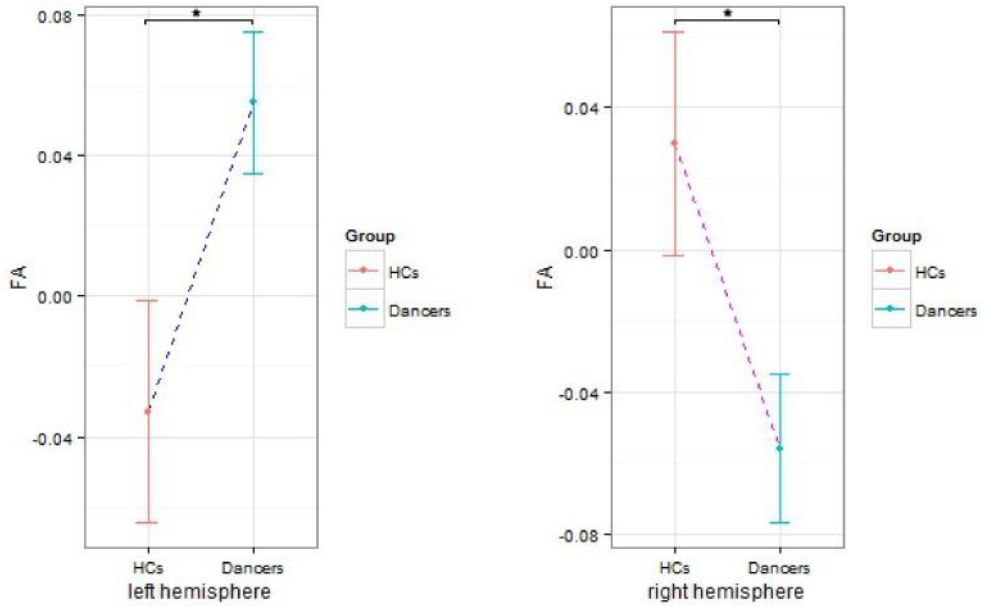

Figure 9. Left: higher L-R FA in dancers relative to HCs, * $p < .10$; right: higher R-L FA in HCs relative to dancers, * $p < .10$. Error bars represent 95% confidence intervals.

Table 2 lists the peak MNI coordinates of the R-L FA analysis, and because this analysis measures bilateral difference of homologous structures between groups, the coordinates are identical to the L-R results but in the right hemisphere . The R-L and L-R p-values, however, differ marginally as then do the number of significant FA, FWE-corrected voxels. Again, as noted previously, both left and right FA values are analyzed in the left hemisphere by the tbss_sym script. This results in negative MNI x-coordinates not just for the left hemisphere but right hemisphere as well. At this exploratory level of significance (α= 0.10), age was negatively correlated with FA lateralization, $r_s = -.55$, $p < .05$, $r_s^2 = .31$. Gender was not correlated with FA lateralization, $r_s = -.33$, $p = .17$, $r_s^2 = .11$. There was a strong, positive correlation between years of dance training experience and FA lateralization, $r_s = .74$, $p < .001$, $r_s^2 = .55$. Correlations were also assessed between (peak) FA values and AD, FA and MD and FA and RD; AD, MD and RD were captured within a 15 mm sphere of MNI max coordinate -15 -56 28. Axial diffusion was not significantly correlated with FA lateralization ($p > .05$), though there was a trend, $r_s = .45$, $p =$

.06, r_s^2 = .20; MD was not correlated with FA lateralization, r_s = -.15, p = .52, r_s^2 = .03; but RD diffusion was negatively correlated with FA lateralization, r_s = -.51, p < .05, r_s^2 = .26.

Table 1.

Dancer vs. HCs (tbss_sym): L – R (dancer leftward FA asymmetry)

Voxels	Max X (mm)	Max Y (mm)	Max Z (mm)	L>R FA structures	*d*	*p* <.10
260	-15	-56	28	JHU: 11% left Ci; JH: 10% left CB	2.00	0.052
49	-17	22	41	HOC: 8% WM of left SFG	1.89	0.079
29	-18	33	31	JHU: 3% left IFOF; 3% left ATR	2.25	0.059
25	-7	-67	34	JHU: 3% left Ci	2.34	0.069
5	-19	27	33	JHU: 3% left ATR; HOC: 4% WM of left SFG	1.19	0.099
1	-14	47	27	JHU: 29% left FMi; 3% left ATR	1.65	0.100

ATR = anterior thalamic radiation; CB= callosal body; Ci = cingulum; *d* = Cohen's *d;* FMi = forceps minor; IFOF = inferior fronto-occiptal fasciculus; ILF = inferior longitudinal fasciculus; SFG= superior frontal gyrus; SLF = superior longitudinal fasciculus; UF = uncinate fasciculus; HCs=healthy controls. Percentages represent the probability that fractional anisotropy (FA) occurs in the associated structure as estimated by HOC= Harvard-Oxford Cortical Atlas, JHU= JHU- ICBM White-Matter Tractography and JH= Juelich Histological Atlases.

Table 2

Dancer vs. HCs (tbss_sym): R-L FA (controls rightward FA asymmetry)

Voxels	Max X (mm)	Max Y (mm)	Max Z (mm)	R>L structures	*d*	*p* <.10
260	-15	-56	28	JHU: 11% right Ci; JH: 10% right CB	2.00	0.053
67	-17	22	41	HOC: 8% WM of right SFG	1.89	0.084
30	-18	33	31	JHU: 3% right IFOF; 3% right ATR	2.25	0.060
27	-7	-67	34	JHU: 3% right Ci	2.34	0.070
15	-19	27	33	JHU: 3% right ATR; HOC: 4% WM of right SFG	1.19	0.096
8	-14	47	27	JHU: 29% right FMi; 3% right ATR	1.65	0.095

ATR = anterior thalamic radiation; CB= callosal body; Ci = cingulum; *d* = Cohen's *d* ; FMi = forceps minor; IFOF = inferior fronto-occiptal fasciculus; ILF = inferior longitudinal fasciculus; WM of SFG= superior frontal gyrus ; SLF = superior longitudinal fasciculus; UF = uncinate fasciculus. Percentages represent the probability that fractional anisotropy (FA) occurs in the associated structure as estimated by HOC= Harvard-Oxford Cortical Atlas, JHU=JHU- ICBM White-Matter Tractography, HOC= Harvard-Oxford Cortical Structural, and JH= Juelich Histological Atlases.

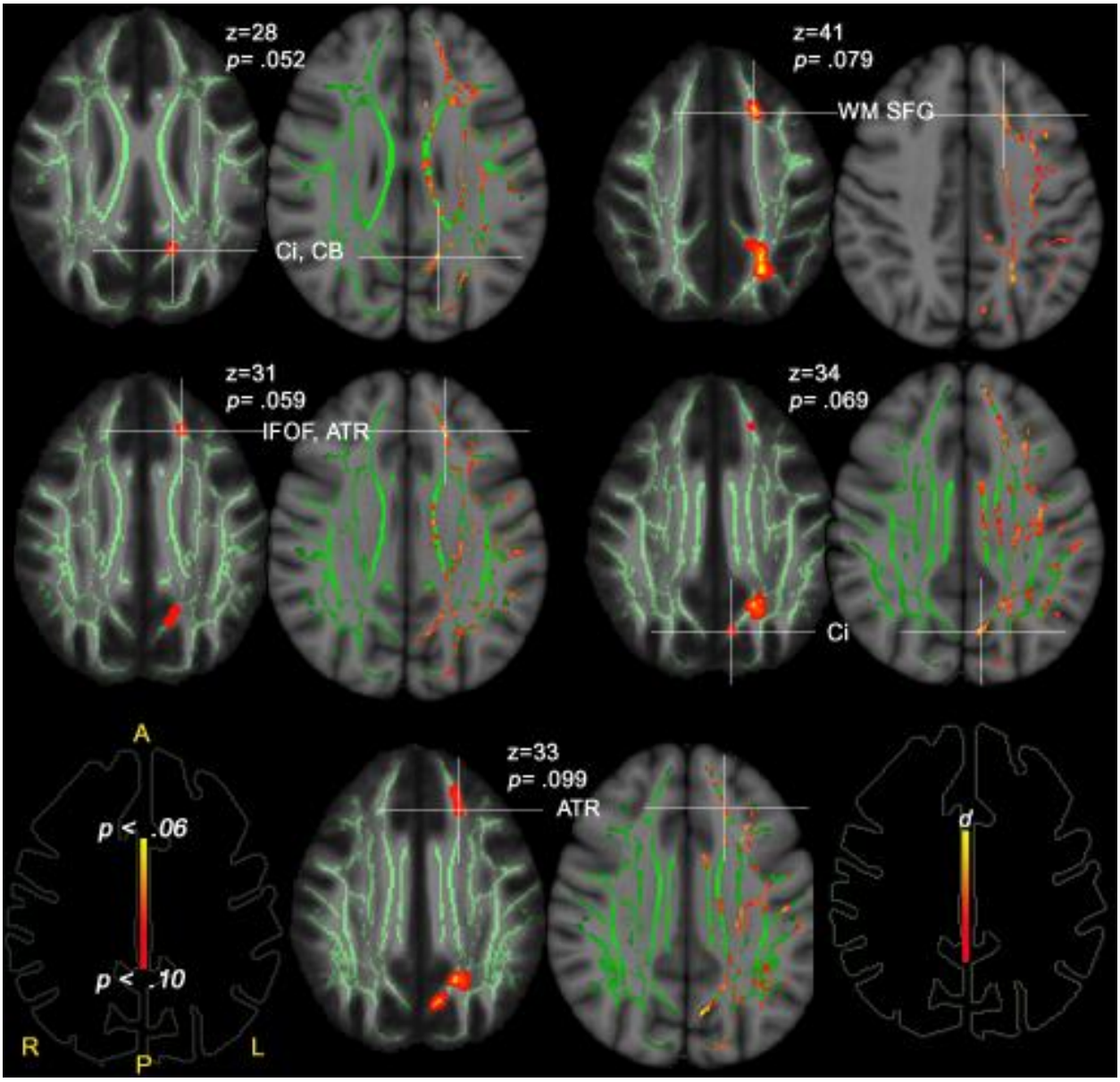

Figure 10. All images display dancer leftward FA asymmetry from tbss_sym analysis. Larger, higher intensity clusters in the top row persist through other layers. Top row: the Ci and CB at max MNI (mm) -15 -56 28 (p=0.052), WM underlying SFG at max MNI -17 22 41 (p= 0.079); 2nd row: the IFOF and ATR at max MNI -18 33 31 (p= 0.059); Ci at max MNI -7 -67 34 (p= 0.069); 3rd row: the ATR at max MNI -19 27 33 (p= 0.099). Significant voxels have been thickened for display using the tbss_fill script. Each axial image is paired with an effect size map; the latter is located on the right of each image pair. The effect size is a Cohen's *d* range of .2 to .8. For viewing purposes the upper *d* limit was adjusted to 1.95 and red-

yellow coded. All images are at $p < 0.10$, FWE corrected. ATR=anterior thalamic radiation; Ci=cingulum; CB= callosal body; IFOF= inferior fronto-occipital fasciculus; SFG=superior frontal gyrus

The TBSS analysis localizing FA differences between-groups demonstrated that dancers had greater left FA ($M = 0.6301 \pm 0.0438$) relative to HCs ($M = 0.5563 \pm 0.0313$) in several structures. This difference was significant, $p < 0.10$, (FWE corrected). Table 3 lists effect sizes (Cohen's d) of significantly different FA voxels and the underlying probable (probability expressed as a percentage) structures of these voxels. Effect sizes are high, even higher than those revealed in the tbss_sym FA lateralization analysis. This indicates a large between group effect of dance training on FA. The graph in Figure 11 characterizes the TBSS script FA results and Table 3 lists all peak MNI coordinates of significantly different voxels. The TBSS analysis images in Figure 12 highlight peak output from the cluster report data of Table 3 and show that a significant FA difference occurred in the left hemisphere, where dancer FA exceeded FA of HCs. The radiological convention axial views are shown and an effect size map with a range of .2 to .8 (Cohen's *d*) is associated with each image. To facilitate the visual differentiation of the range of effect sizes, the upper level of the effect size range was set to 1.95. As reiterated previously, this is a visual aid only and does not alter the actual effect sizes. Images in Figure 12, like those in Figure 10, are arranged in ascending order from smallest p-value (top) to largest p-value in the last row. This follows the order of clusters in Table 3. Also as in Figure 10, in Figure 12 the larger clusters of the top rows, which have MNI max coordinates with lower p-values, generally persist in the MNI coordinates with higher, less stringent p-values. The first and largest cluster in Table 3, MNI -27 -26 17, has the lowest MNI max coordinate p-value. This largest cluster of significant voxels was identified as within the CST by reference to the JHU White-Matter Tractography Atlas (16% probability) and Juelich Histological Atlas (27% probability). The Juelich Histological Atlas also identified this cluster as including the SLF (35% probability). The first row of Figure 13 consists of all 3 cardinal views of the largest and most significant cluster at MNI max coordinates -27 -26 17. The 2nd row adds an atlas based mask (JHU White-Matter Tractography Atlas) of the CST which visually appears to corroborate that

some portion of these voxels represent CST fibers. Figure 14 provides a 3D depiction of this significantly greater left CST/SLF FA coordinate in dancers at $p < 0.062$ (the lowest p-value in the TBSS analysis). The Juelich Histological Atlas indicates that some part of this group of FA voxels may also partially lie in the SLF; perhaps within the AF segment of the SLF depicted by Catani et al (2007 [see Figure 4]). However, as shown in the 3rd row of Figure 13, an added SLF mask (Juelich Histological Atlas) reveals an unconvincing picture of substantive SLF involvement with this cluster at $p = 0.062$; an impression also conveyed by Figure 14. Interestingly, lowering the threshold to $p < 0.10$ (the initial base alpha level for this analysis) the involvement of the SLF, and potentially the AF segment of the SLF, appears evident as revealed in the Figure 15 3D image. Age was not correlated with greater FA in dancers, $r_s = -.40$, $p = .10$, $r_s^2 = .16$. Gender was not correlated with greater FA in dancers, $r_{pb} = -.16$, $p = .53$, $r_{pb}^2 = .02$. However, there was a strong, positive correlation between years of dance training experience and greater FA in dancers, $r_s = .65$, $p < .01$, $r_s^2 = .42$. Correlations were also assessed between (peak) FA values and AD, FA and MD and FA and RD; AD, MD and RD were captured within a 15 mm sphere of MNI max coordinate -27 -26 17 delimiting the region of dancer greater left CST/SLF FA. There was a large, positive correlation between greater FA in dancers and AD, $r = .62$, $p < .01$, $r^2 = .39$; but a negative correlation between greater FA and RD, $r = -.61$, $p < .01$, $r_s^2 = .36$. There was no correlation between greater FA in dancers and MD, $r = .09$, p .74, $r^2 = .01$.

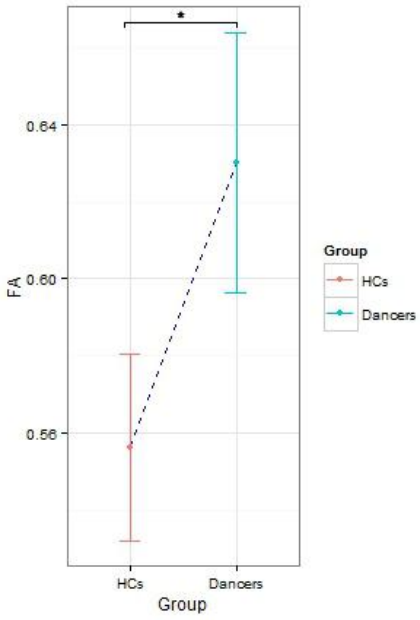

Figure 11. Greater FA in dancers relative to HCs localized to the left hemisphere. Error bars represent a 95% CI; * $p < 0.10$

Table 3.

Dancer vs. HCs (TBSS): greater dancer left hemisphere FA

Voxels	Max X (mm	Max Y (mm	Max Z (mm)	Structures	*d*	*p* <.10
532	-27	-26	17	JH: 35% left SLF, 27% left CST; JHU 16% left CST	3.15	0.0624
136	-24	22	13	JHU: 29% left IFOF; 19% left UN; 13% left ATR; 3% left SLF	2.35	0.0812
61	-40	-43	14	JHU: 21% left SLF (temp); 21% left SLF; JH 5% left OR	2.28	0.0876
47	-23	28	0	JHU: 26% left IFOF; 22% left UN; 8% left ATR	2.19	0.0882
10	-35	-43	13	JHU: 16% left ILF: 11% left SLF; 8% left SLF(temp); 5% left IFOF; JH: 63% left OR; 11% CB	2.07	0.0894

ATR = anterior thalamic radiation; CB= callosal body; Ci = cingulum; *d* = Cohen's *d* ; FMi = forceps minor; IFOF = inferior fronto-occiptal fasciculus; ILF = inferior longitudinal fasciculus; OR= optical radiation; SFG= superior frontal gyrus ; SLF = superior longitudinal fasciculus; UF = uncinate fasciculus. Percentages represent the probability that fractional anisotropy (FA) occurs in the associated structure as estimated by JHU=JHU- ICBM White-Matter Tractography, and JH= Juelich Histological Atlases.

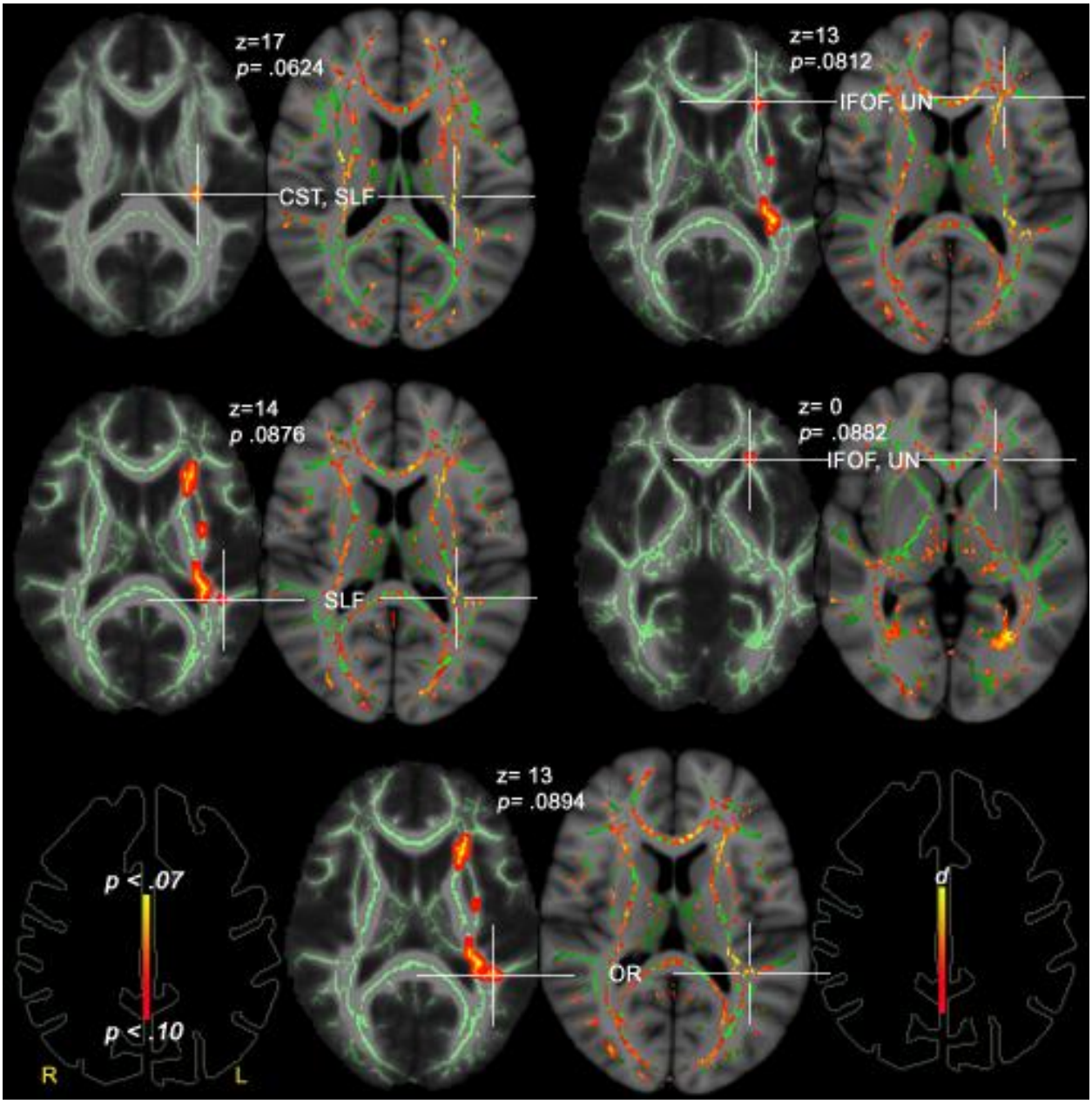

Figure12. All images are from the TBSS analysis; greater dancer FA is demonstrated localized to the left hemisphere. Larger, higher intensity clusters in the top row persist through other layers. Only the two structures with highest identification probability are referenced here. Top row left: SLF and CST at max MNI (mm) -27 -26 17 (p =0.0624); top row right cluster: IFOF, UN at max MNI -24 22 13 (p= 0.0812); 2nd row left: the SLF (temp) and SLF at max MNI -40 -43 14 (p =0.0876); 2nd row right: IFOF and UN at max MNI -23 28 0 (p= 0.0882); 3rd row: WM OR at max MNI -35 -43 13 (p=0.0894). Significant voxels

have been thickened for display using the tbss_fill script. Each axial image is paired with an effect size map; the latter is located on the right of each image pair. The effect size is a Cohen's *d* range of .2 to .8. For viewing purposes the upper *d* limit was adjusted to 1.95 and red-yellow coded. All images are at $p < 0.10$, FWE corrected. Atlases used: JHU=JHU- ICBM White-Matter Tractography Atlas, and JH= Juelich Histological Atlas. ATR=anterior thalamic radiation; Ci=cingulum; CB= callosal body; CST= corticospinal tract; IFOF= inferior fronto-occipital fasciculus; OR= optic radiation; SFG=superior frontal gyrus; WM= white matter.

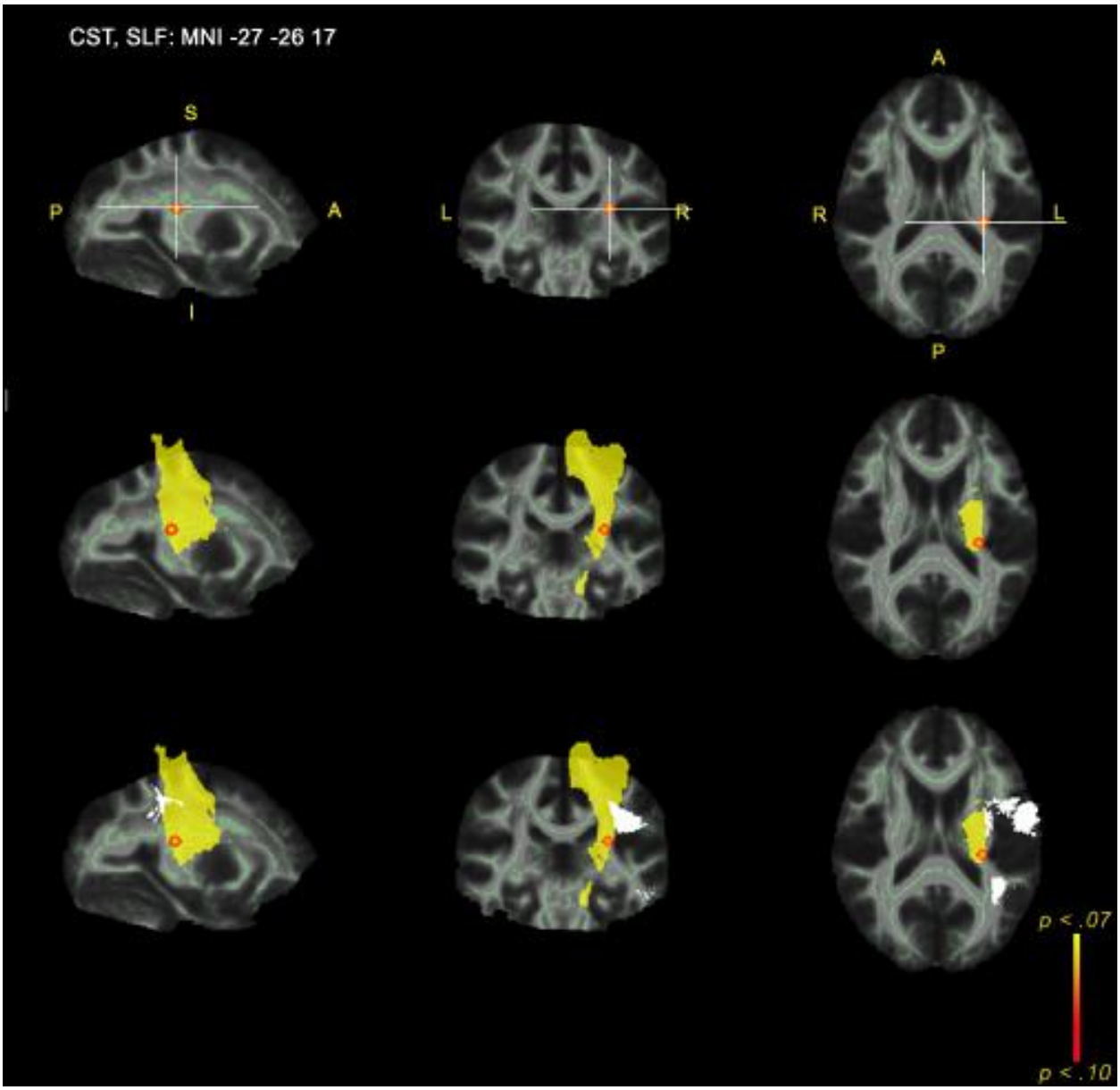

Figure 13. Shown in the first row are 3 cardinal views of the TBSS analysis image of the voxels with the greatest statistical level of significance (p= 0.0624) at the cluster with MNI max coordinates -27 -26 17 (CST and SLF) which is the largest cluster in Table 3. The 2nd row adds an atlas based mask (JHU White-Matter Tractography Atlas) of the CST (yellow). The 3rd row adds an SLF white mask (Juelich Histological Atlas) to the images shown in the first row. CST= corticospinal tract; SLF= superior longitudinal fasciculus.

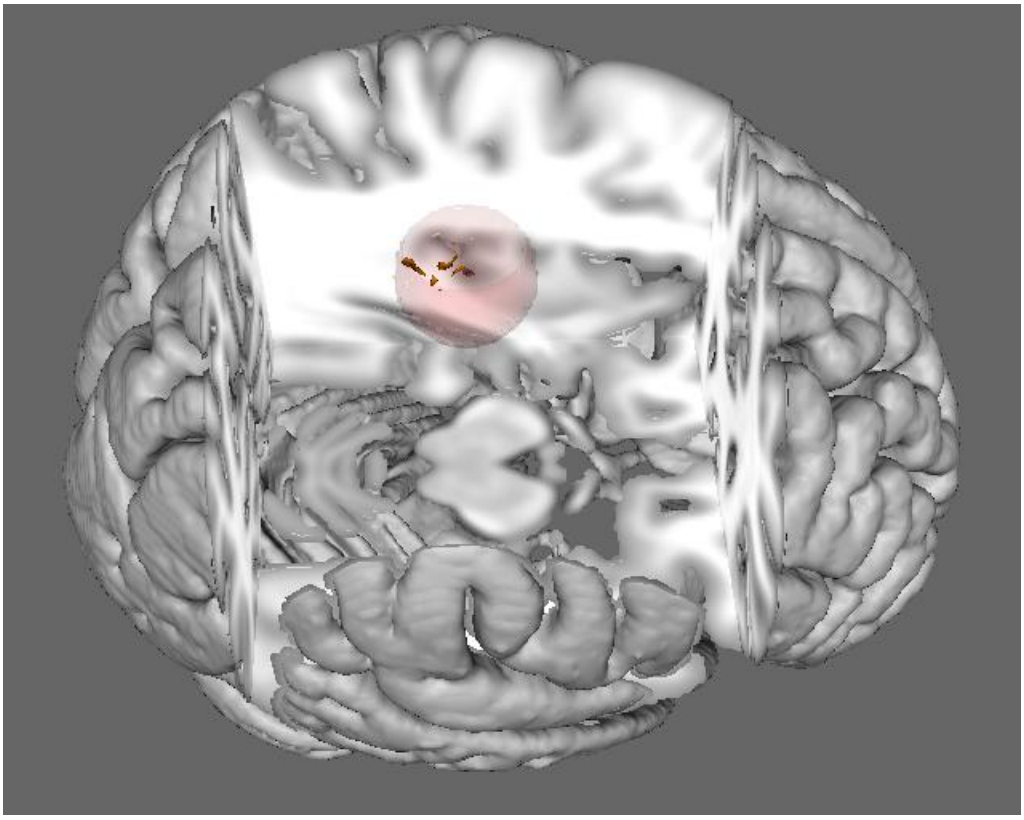

Figure 14: TBSS derived 3D depiction of greater left CST/SLF FA in dancers at $p < 0.065$. This area of significantly greater leftward FA in dancers (encompassed by a sphere at 90% transparency) extends out 15 mm (radius) from center MNI max coordinate -27 -26 17 to form a sphere.

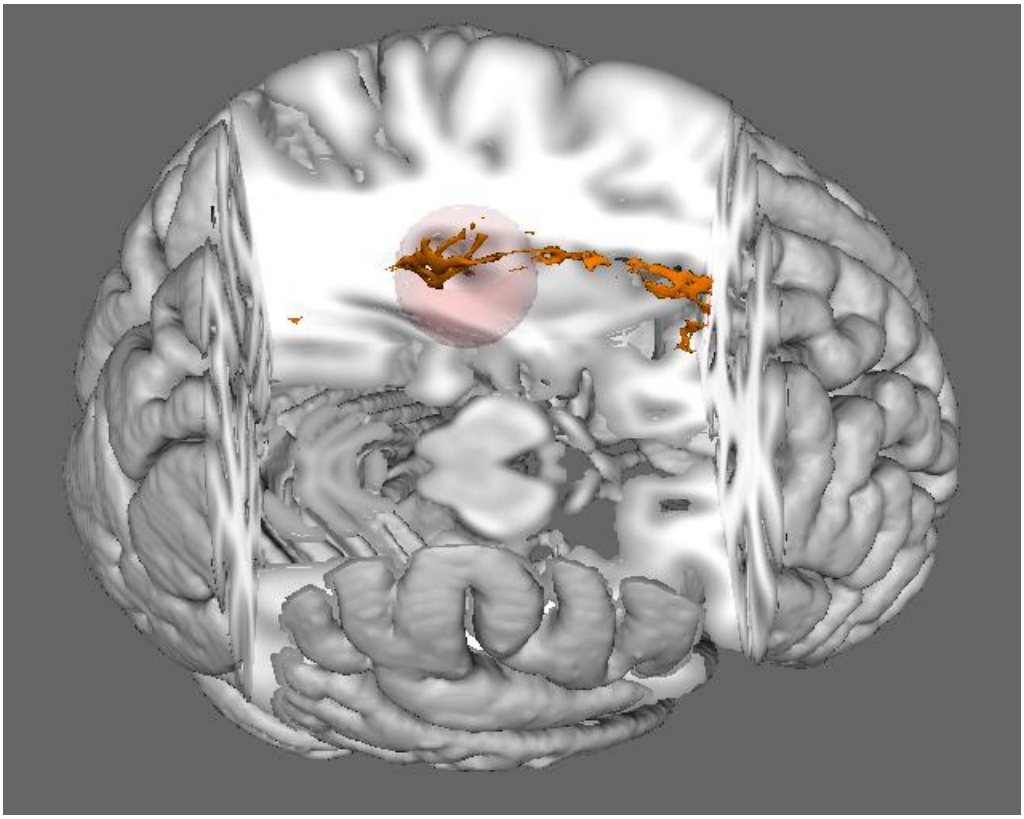

Figure 15: TBSS derived 3D depiction of greater left CST/SLF FA in dancers at $p < 0.10$. At this level of significance, involvement of the SLF in addition to the CST at MNI max coordinate -27 -26 17 appears evident.

To test for between group differences at the standard and more stringent significance level, both the tbss_sym and TBSS analyses were thresholded at $\alpha = 0.05$. The tbss_sym analysis revealed a significant difference between groups at the MNI max coordinates (mm) of -21 -55 39, $p = .038$ (FWE corrected), $d = 1.83$. The cluster with the latter MNI max coordinates consisted of 48 significantly different voxels and was identified with 3% probability of being the ATR by reference to the JHU White-Matter Tractography Atlas. All three cardinal views of the putative ATR cluster of dancer leftward FA asymmetry are shown in Figure 16. The third row of Figure 16 displays a Cohen's *d* effect size map ranging from .2 to .8, with the upper *d* limit adjusted, for viewing purposes only, to 1.95 and red-yellow coded. A posterior aspect of the ATR in this location appears consistent with the results of Wakana et al.

(2007) reproduced in Figure 18. This cluster of 48 significantly different voxels demonstrated leftward FA asymmetry for dancers relative to HCs. The R-L FA analysis thresholded at 0.05, as expected, revealed rightward FA asymmetry for HCs at the same MNI location but in the right hemisphere ($p <$ 0.05, FWE corrected). Images for R-L rightward ATR FA asymmetry in HCs relative to dancers are not shown (they are identical to the L-R leftward FA asymmetry images of the ATR in Figure 16). As shown in second row of Figure 16, the 48 voxel cluster with MNI max coordinates (mm) of -21 -55 39, identified with 3% probability of the being the ATR, is surrounded by an atlas-based (Juelich Histological Atlas) mask of the anterior intra-parietal sulcus (hIP3). The image in Figure 17 provides a 3D perspective of the cluster centered at MNI max coordinate -21 -55 39. At $\alpha = .05$ (and as occurred at $\alpha = .10$) age was negatively correlated with FA lateralization, $r_s = -.62$, $p < .05$, $r_s = .39$. Gender was not correlated with FA lateralization, $r_{pb} = -.21$, $p = .40$, $r_{pb}^2 = .04$. There was a positive correlation between years of experience and FA lateralization, $r_s = .55$, $p < .05$, $r_s^2 = .30$. Correlations were also assessed between (peak) FA values and AD, FA and MD and FA and RD; AD, MD and RD were captured within a 15 mm sphere of MNI max coordinate -21 -55 39. There was a strong, positive correlation between FA lateralization and AD, $r = .76$, $p < .001$, $r^2 = .57$, but an equally strong negative correlation between FA lateralization and RD, $r = -.78$, $p < .001$, $r^2 = .61$. There was no correlation between FA lateralization and MD, $r_s = .11$, $p = .66$, $r_s^2 = .01$.

At $\alpha = 0.05$ there were no significantly different voxels in the TBSS analysis – neither group demonstrated greater FA at this level of significance. However there was a trend of significantly different voxels at MNI max coordinate -27 -26 17, $p = 0.06$, $d = 3.15$. This is the same cluster reported at $p < 0.10$ and listed at the top of in Table 3 and in the top row of Figure 13. As noted previously, portions of the cluster were identified as lying within the CST (JHU White-Matter Tractography Atlas and Juelich Histological Atlas) and the SLF (Juelich Histological Atlas).

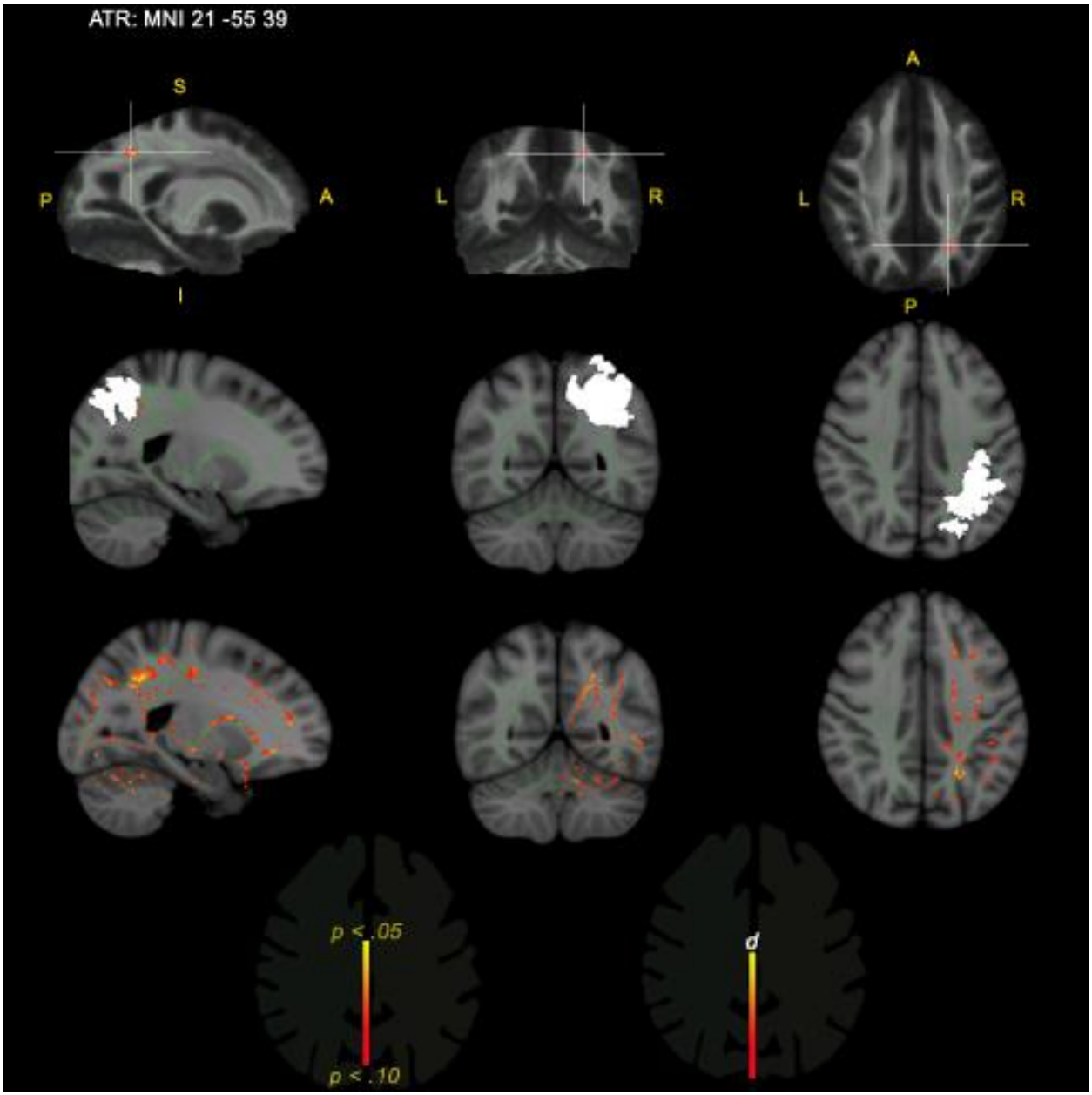

Figure 16. Top row: 3 cardinal views of the posterior aspect of the ATR, MNI max coordinates (mm) of -21 -55 39; 2nd row: a mask of the anterior intra-parietal sulcus (hIP3) is applied to all 3 cardinal views; 3rd row: Cohen's *d* image range .2 to 1.95. ATR= anterior thalamic radiation

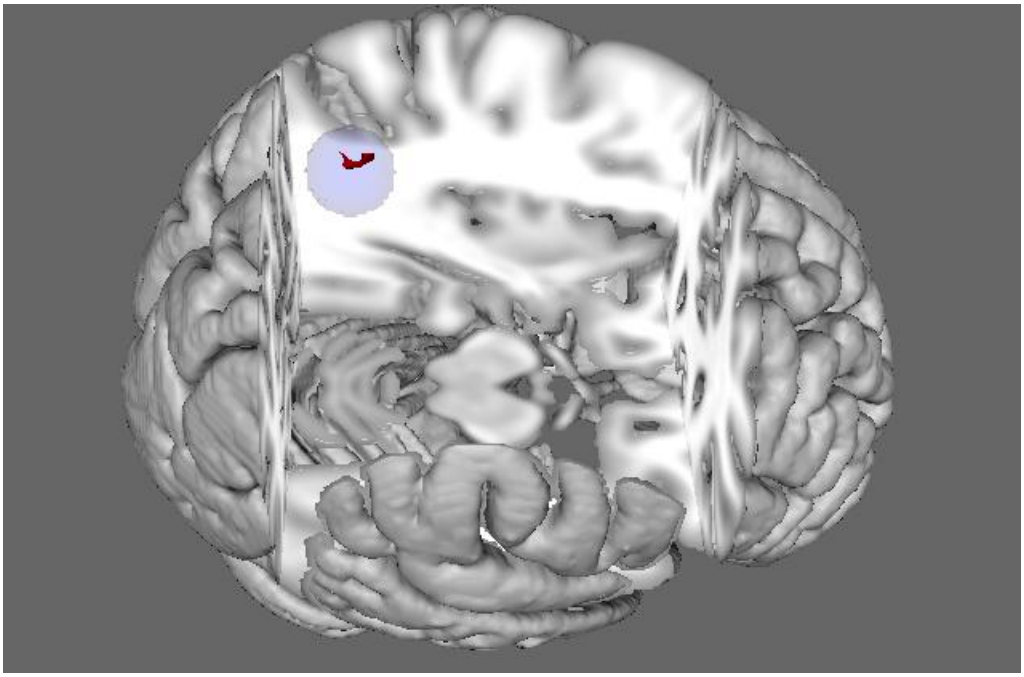

Figure 17: Tbss_sym derived image of dancer leftward FA centered at MNI max coordinate -21 -55 39; putative ATR (3% probability, JHU White-Matter Tractography Atlas). ATR= anterior thalamic radiation

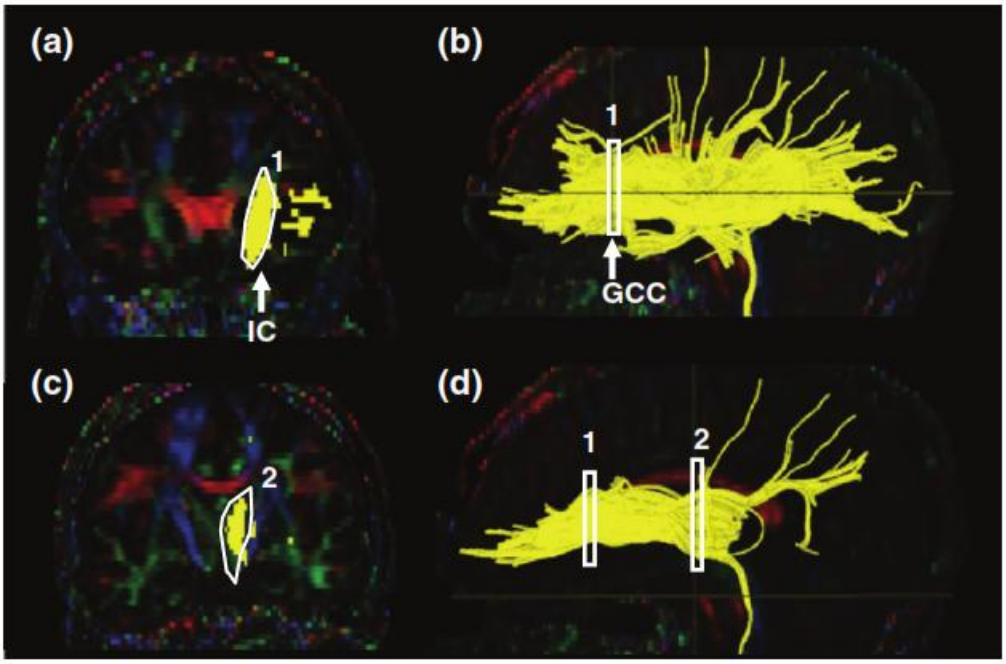

Figure 18. Tractography of the ATR reprinted from Wakana et al. (2007). The numbers 1 and 2 represent ROIs for the ATR; (a) and (c) are coronal sections and (b) and (d) are mid-sagittal sections: ATR=anterior thalamic radiation; IC= internal capsule; GCC= genu of the corpus callosum.

Chapter Four

4.1 Discussion

In keeping with the order of analyses, the global histogram assessment of FA distribution will be discussed first, followed by the global FA and tbss_sym FA analyses for each group. Subsequently, the between group volumetric and between group FA results from both the tbss_sym and TBSS analyses will be discussed. The Global histogram derived from skeletonized FA mean image of dancers and HCs showed relatively normal distribution shape based on a Lilliefors (1967) analysis (see bottom row of Figure 5) indicating that the TBSS mean FA skeleton produced a relatively normal FA distribution that did not compromise the accuracy of t-tests (Welch) used for the global FA and volumetric analyses, which did not use the permutation analysis employed in the tbss_sym FA and TBSS analyses. As noted in the results, additional indices of relative distribution normality were also employed prior to the global FA volumetric tests and there was no evidence of violations of normality.

For dancer and HCs groups the tbss_sym analysis localized absolute leftward and rightward FA asymmetry in structures; the global FA calculation simply summed total leftward and rightward FA. To identify asymmetry in as many structures as possible, the liberal $\alpha = 0.10$ level of significance was used in the tbss_sym analysis. The standard level of significance (0.05) was used in the global FA analysis. Otherwise, the global FA and tbss_sym analyses for dancer and control groups were very similar tests with similar outcomes: both calculated if L-R FA and R-L FA differed from zero and was positive, both demonstrated a high extent of leftward FA lateralization. The similarity of outcomes can be seen in Figures 6 and 7 which show the patterns for global FA and tbss_sym FA respectively. Of course, the summed global FA values are much higher than the localized FA values of the tbss_sym analysis. The global FA and tbss_sym FA test results were, as expected, highly significant. In the global FA analyses, L-R FA and R-L FA significantly differed from zero and were positive for dancers ($p < 0.0001$) and HCs ($p < 0.0001$). Similarly, the tbss_sym analyses demonstrated that L-R FA and R-L FA significantly differed from zero and were positive for dancers ($p < 0.10$) and HCs ($p < 0.10$). In addition, in both tests, for both groups the mean left FA was significantly greater than the mean right FA: for global FA this is

conveyed by the non-overlapping boxplot notches in Figure 6, where left FA is clearly higher; in respect to the tbss_sym analysis this is conveyed by the non-overlapping error bars in Figure 7, and again left FA is clearly higher than right FA. From the tbss_sym analysis, structures with dancer L>R FA included the IFOF and a posterior aspect of the ATR (see Table 1, Appendix A for a list of probabilistic structures); structures with controls L>R FA included the uncinate and IFOF (see Table 2, Appendix A for a list of probabilistic structures). Structures of R>L FA for both groups are not listed but available on request. In summary, these tests demonstrated definitive leftward FA lateralization for both groups. At the time of this writing, there were no comparable training related studies published involving 1-sample global and tbss_sym FA analyses. These tests, however, were insightful: they demonstrated the overall pattern of leftward FA asymmetry putatively revealing the dominance of left hemisphere WM structures in both groups.

Turning to the volumetric data, there are several studies (most of which were cited in the introduction) that reported a training effect on regional brain volume (mainly GM volume). Regional as well as global volume results have also been specified in training related research (Hanggi et al., 2010; Maguire et al., 2000). The current study calculated only training-associated global volume alteration. Of course, while brain metrics such as global FA asymmetry and global volume provide useful gross measurements, such constructs are blind to regional differences. The self-evident disparity between global and regional test methods makes drawing analogies between outcomes of the two methodologies potentially misleading: a reported virtual island of regional volume alteration may exist in a sea of global antithetical volume alteration. Because of the fundamental difference between global and regional analyses, comparisons between current study global volume findings and regional-only volume findings in the literature must be regarded with caution.

Bearing this in mind, the between-group global volumetric analysis in the current study demonstrated that dancers had greater global WM ($p < 0.05$, r^2=.25) volume (see Figure 8, left); gender and age were not correlated with greater global WM volume in dancers, but there was a large, positive

correlation between years of dance training experience and greater WM volume in dancers, ($p < .05$, $r_s^2 = .31$). This global finding appears in stark contrast with the lower global and regional dancer WM volumes reported by Hanggi et al (2010) but consistent with the aerobic-training associated increase in regional WM reported by Colcombe et al. (2006) and increased bilateral WM AF tract volume of musicians, most pronounced in the left hemisphere, reported by Halwani et al. (2011).

Similar to the global WM findings, the global GM results revealed dancers had significantly higher GM volume ($p < 0.01$, $r^2 = .36$) than HCs (see Figure 8, right). These results are in concert with most GM regional results for trained groups in the literature which emphasize mainly regional brain volume increases (Boyke et al., 2008; Colcombe et al., 2006; Draganski et al., 2004; Hufner et al., 2010 Maguire et al., 2000; Taubert et al., 2010), though antithetically two of the three dancer studies (Hanggi et al., 2010; Nigmatullina et al., 2013), reported largely reduced GM structure. The other dancer study, Hufner et al., 2010, reported dance training-related increases in GM volume. In the current study, gender was not correlated with GM global volume, but there was a strong positive correlation between years of training experience and higher global GM in dancers, $r_s = .61$, $p < .01$, $r_s^2 = .38$. In addition, there was also a strong negative correlation between age and gobal GM, $r_s = -.69$, $p < .01$, $r_s^2 = .48$. A negative correlation between age and GM volume is consistent with previous research (Giorgio et al., 2010).

At the significance level of $\alpha = 0.10$, the tbss_sym and TBSS analyses both demonstrated left-centric FA in dancers. The L-R FA asymmetry analysis (tbss_sym) localizing bilateral FA differences between-groups revealed that dancers had higher leftward FA relative to HCs in specific structures, and HCs had higher rightward FA in the homologous structures of the right hemisphere ($p < 0.10$, FWE corrected). Greatest lateralization occurred in aspects of the cingulum and callosal body. There was a trend of AD correlation with FA ($p = .06$, $r_s^2 = .20$) lateralization, and there was a negative correlation between RD and FA lateralization ($p < .05$, $r_s^2 = .26$). There was a large positive correlation ($p < .001$, $r_s^2 = .55$) between years of experience and FA lateralization and a large negative correlation between age and FA lateralization ($p < .05$, $r_s^2 = .31$).

At the significance level of α= 0.10, the TBSS analysis localizing absolute FA differences between-groups demonstrated that dancers had greater left FA relative to HCs in specific structures ($p <$ 0.10, FWE corrected). Higher dancer FA was localized with greatest significance to areas of the CST and SLF. Within a sphere of 15 mm radii centered at the CST/SLF MNI max coordinate -27 -26 17, there was a large, positive correlation between greater FA in dancers and AD ($p < .01$, $r^2 = .39$); but a negative correlation between greater FA and RD ($p < .01$, $r_s{}^2 = .36$). Also, there was a large positive correlation between years of dance experience and greater dancer FA ($p < .01$, $r_s{}^2 = .42$).

The graph in Figure 11 is similar to the pattern of the tbss_sym analysis in the Figure 9 left graph in so far as both graphs show left-centric FA. However, while both analyses employ a permutation-based t-test as the statistical test proper, tbss_sym and TBSS analyses are different tests using different scripts. Outcomes therefore are not directly comparable, which is conveyed, in part, by the widely differing FA ranges of the tbss_sym (Figure 9) and TBSS (Figure 11) between group analyses, and more obviously by the differing tbss_sym analysis results listed in Table 1 and the TBSS analysis results listed in Table 3 (all tables list peak MNI coordinates). Each test contributes a different characteristic of FA between groups putative neural asymmetry. The tbss_sym script reveals the bilateral FA difference in left and right hemisphere of homologous structures; because this is a left vs right (L-R) hemisphere difference, positive FA values in one hemisphere correspond with negative values in the like structures of the other hemisphere. This is shown in Figure 9. The latter figure indicates that at α= 0.10, in a given structure, ballet dancers had higher L-R FA relative to HCs, whom, while having lower L-R FA than dancers, had higher R-L FA. Table 1 lists the structures for dancer higher L-R or leftward FA (the same structures for HCs R-L FA listed in Table 2) and Figure 10 displays the axial localization of these significantly different FA coordinates. The largest cluster of significantly different FA voxels, which also had the lowest p-value ($p < 0.052$, FWE corrected, $d= 2.0$), was located at MNI max coordinates -15 -56 28. This cluster had an 11% probability of including posterior cingulum fibers (JHU White-Matter Tractography Atlas) and a 10% probability of including the callosal body (Juelich Histological Atlas). The aforementioned cluster is localized in the first row of Figure 10. Effect sizes of structures shown in Figure 10 and listed in Table 1

were large ($d > 0.8$), indicating a strong and meaningful lateralization effect for dancer and control populations; leftward asymmetry in dancers but rightward asymmetry in controls. As mentioned previously, there is an absence of comparative tbss_sym training related data in the literature, but in a tbss_sym analysis of a normal, large untrained group (857), Takao et al. (2012) reported asymmetries including parts of the cingulum and callosal body.

In contrast to the tbss_sym script, the TBSS script, as noted above, provides an absolute measure of FA (typically 0 to 1). The FA values from the TBSS analysis in Figure 11 are much higher than the tbss_sym FA values in Figure 9 because they don't represent a bilateral difference. The disparity in the range of FA values between the two differing analyses is most evident in Figure 19, which simply plots the mean FA values from tbss_sym and TBSS analyses. Figure 20 similarly characterizes inter-test disparity in FA ranges using density plots, but FA values are also further broken-down in each analysis by group.

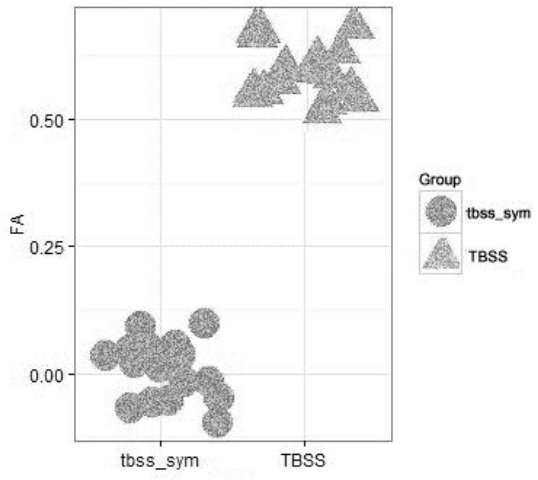

Figure 19. Mean tbss_sym (L-R) and TBSS FA values

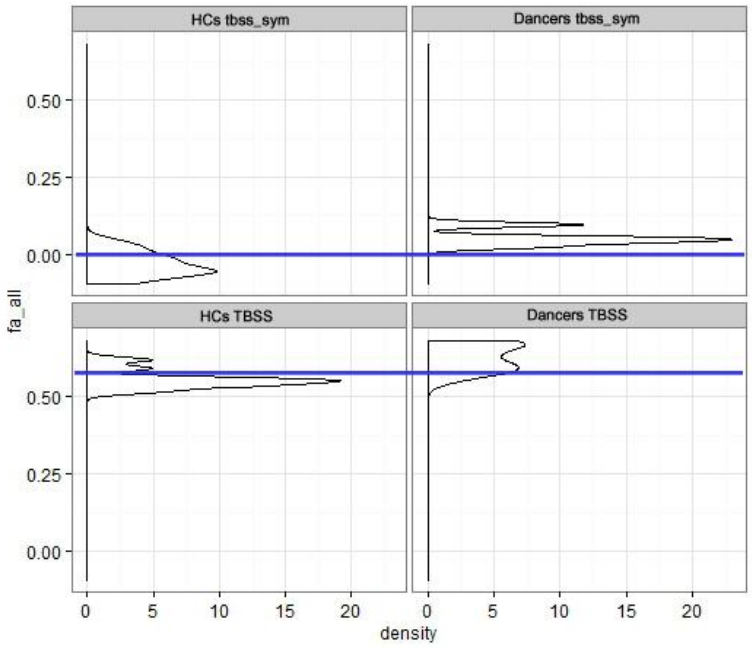

Figure 20. Top row: tbss_sym (L-R) mean FA, HCs left and dancers right; 2nd row: TBSS mean FA values, HCs left and dancers right. HCs=healthy controls.

As Figure 11 indicates, dancers had significantly greater FA localized in left hemisphere structures. Table 3 lists all TBSS peak MNI coordinates of significantly different voxels with their effect size; the images in Figure 12 highlight localization of these clusters of significant voxels. The first and largest cluster of significantly different voxels (p= 0.06, FWE corrected, d= 3.15) in Table 3, MNI -27 -26 17, had the lowest p-value in the TBSS analysis and was identified as within the left CST by reference to the JHU White-Matter Tractography Atlas (16% probability) and Juelich Histological Atlas (27% probability). The Juelich Histological Atlas also identified this cluster as including the left SLF fibers (35% probability). Figure 13 consists of all 3 cardinal views of this largest of Table 3 clusters (MNI mm -27 -26 17) with an added atlas based mask (JHU White-Matter Tractography Atlas) of the CST (2nd row) which circumscribes the cluster and provides additional visual corroboration that some portion of these voxels of FA represent underlying significantly different left CST fibers in dancers. A 3D perspective of the putative CST involvement is provided by Figure 14. An atlas based SLF mask (Juelich Histological

Atlas) is also shown in Figure 13 (3rd row) but visual inspection imparts little confidence that there is substantial SLF fiber involvement with this cluster of voxels at $p = 0.062$. As noted in the results, by thresholding this image at $\alpha=0.10$ (the base alpha level for this analysis) the involvement of the SLF, and potentially the AF segment of the SLF, is vividly suggested (see Figure 15). However, given that at least 2 different fiber tracts cross in 1/3rd of voxels (Tuch et al., 1999) and fiber tracts intersect frequently, definitively establishing tract fiber identity can be problematic especially in areas of crossing fibers. As such, it is acknowledged that probabilistic tractography, not conducted here, would have further substantiated identification of tracts underlying significantly different FA. Effect sizes of structures analyzed by the TBSS script, shown in Figure 12 and listed in Table 3, were large (d >0.8) indicating a dance training effect of high magnitude. The average of effect size peak values in Table 3 from the TBSS script analysis was ~ 24% higher than the average of the tbss_sym effect size of peak values in Table 1. This suggests that the magnitude of the FA between groups difference revealed by the TBSS script exceeded the magnitude of the FA difference between sides (lateralization) revealed by the tbss_sym script.

Most training research assessing the FA metric has reported regional training-dependent increased FA (Bengtsson et al., 2005; Keller & Just, 2009; Halwani et al., 2011; Scholz et al., 2009; Schmithorst & Wilke, 2002; Takeuchi et al., 2010; Wang et al., 2012). As noted in the latter paragraph and in the results, the TBSS script analysis demonstrated greater left hemisphere FA in the structures of dancers listed in Table 3, mainly in the CST, SLF, inferior frontal occipital fasciculus, uncinate, and ATR. The finding of greater CST FA in dancers of the current study is consistent with greater CST FA reported in world class right-handed gymnasts by Wang et al. (2012), though in the current study greater dancer CST FA was localized in the left hemisphere while in the Wang et al. (2013) study greater FA occurred bilaterally in CST of the gymnasts. The Wang et al. study also reported reduced lower RD in the CST of the gymnasts, which is consistent the high negative correlation of RD with FA found in the current study. Bengtsson et al. (2005) reported higher FA of right-handed musicians in the right posterior limb of the internal capsule, which includes CST fibers. While this is a training associated increase consistent with

the current study, it occurred in the right hemisphere which is antithetical to the current study outcome of heightened left hemisphere CST FA in dancers. Moreover, reports of training-induced reductions in CST FA add to the inconsistent characterization of training effect in terms of the FA metric. Imfeld et al. (2009) reported reduced FA bilaterally in the CST of right-handed musicians and Jancke et al. (2009) reported reduced bilateral FA in the CST of professional golfers. Hanggi et al. (2010) reported lower bilateral FA in the WM serving the premotor cortex, which would include CST fibers. In respect to the SLF, which as noted in the preceding paragraph may underlie a portion of the differing FA voxels in the current study, Halwani et al. (2011) reported higher FA bilaterally in the AF segment of the SLF in musicians. This reported training-related SLF FA increase was bilateral whereas in the current study it was restricted to the left hemisphere. Nevertheless, this Halwani et al. finding is consistent with the current study in so far as both studies found incremental training-related FA in a portion of the SLF.

While both the tbss_sym and TBSS analyses demonstrated between group significant FA differences at the exploratory significance level of α=0.10, only the tbss_sym analysis registered a between group difference at the traditional significance level of α=0.05. In the tbss_sym analysis, and at α=0.05, one cluster of 48 significant voxels ($p < 0.05$, FWE corrected, $d = 1.83$) survived located in a posterior part of the ATR (3% probability of ATR fibers: JHU White-Matter Tractography Atlas). The image of this cluster is shown in Figures 16 and 17. From the volume of 369 significant voxels at =0.10, this represented ~ 154 % drop in surviving significantly different FA voxels. At α=0.05, the tbss_sym lateralization analysis revealed significantly higher leftward ATR FA in dancers and therefore significantly higher right hemisphere ATR FA in HCs ($p < 0.05$, FWE corrected, $d = 1.83$). The cluster of significantly different voxels centered at the ATR and located in the posterior aspect of the ATR is plausibly consistent with ATR projections from the internal capsule reported by Wakana et al. (2007) and reproduced in Figure 18. The 48 voxel cluster of dancer leftward FA (MNI -21 -55 39), is circumscribed by an atlas based (Juelich Histological Atlas) mask of the anterior intra-parietal sulcus (hIP3), which implicates this cluster and adjacent intra-parietal structures in FA alterations related to ballet training. Cortical structures found in this location include the superior parietal lobe, precuneus, lateral occipital

cortex, and supramarginal gyrus (Harvard-Oxford Cortical Structural Atlas). Within a sphere of 10 mm radii centered at the ATR MNI max lateralization coordinate -21 -55 39, there was a large positive correlation between FA lateralization and AD ($p < .001$, $r^2 = .57$), but a large negative correlation between FA lateralization and RD ($p < .001$, $r^2 = .61$). Years of training experience was positively correlated with FA lateralization ($p < .05$, $r_s{}^2 = .30$) and age was negatively correlated with FA lateralization ($p < .05$, $r_s = .39$). As reiterated previously, there is an absence of comparative tbss_sym training related data in the literature from which to gauge the consistency of this and the other tbss_sym findings reported here. As noted previously, at $\alpha = 0.05$ there were no significantly different voxels in the TBSS analysis. However there was a trend of significantly different voxels at CST/SLF MNI max coordinate -27 -26 17, ($p = 0.06$, $d = 3.15$). This is the same cluster listed at the top of in Table 3 and shown in Figures 13 and 14.

The divide in training-induced FA results in the literature may reflect heterogeneity of populations and sample sizes as well differing analysis methods. However, as well documented in a recent meta-analysis (Patel, Spreng, & Turner, 2013), functional magnetic resonance imaging (fMRI) literature also shows divided training effect results, albeit as demonstrated in brain activity increases and decreases rather than structural changes. It seems that the phenomenon of dual increases and reductions in structural and functional parameters is a common property of neuroplastic reorganization induced by training rather than simply the result of heterogeneity of populations, sample sizes and analysis methods.

While FA is a highly sensitive metric of neural diffusivity strength and ostensibly underlying tract integrity, it can not convey the direction of the neural signal flow between cortical or subcortical areas (Huettle, Song & McCarthy, 2008). For example, in the present study context, the leftward FA was found in a posterior aspect of the ATR of dancers and greater dancer CST and SLF FA was localized to the left hemisphere. But this data provides no insight into direction of neural signal flow between these tracts and other structures in their vicinity, and therefore also no indication if direction of signal flow is altered in dancers relative to controls; information which appears critical to understanding the properties and processes involved in the neural network change attending training, or for that matter pathology. Insight

into such mechanisms will undoubtedly largely be revealed as their molecular underpinnings are unraveled. But as this is not likely to be achieved in the short term, more research that combines both structural and functional analyses (Andrews-Hanna et al., 2007; Madden et al., 2004) may be advantageous in linking patterns of structural and functional measurements to behavior. Moreover, and as articulated in a recent paper (May, 2011), the overwhelming majority of training studies in the literature are cross-sectional rather than longitudinal. All the studies reviewed in the introduction, with three exceptions (Draganski et al., 2004; Scholz et al., 2009; Taubert et al., 2010), were cross-sectional (one time point). Longitudinal investigation of structural metrics, such as FA, over a sequence of appropriate time points has greater statistical power (given the reduced variability of repeated-measures analysis) and hence greater promise to reveal, with higher precision, the patterns of structural alterations linked to behavior such as training.

4.2 Limitations

Limitations of this study include the small sample size of 18 (*n*= 9 dancers; 9 controls), a lack of probabilistic tractography, and an absence of regional volumetric analysis. To achieve 80% power and a large effect size at a significance level of .05 a number of at least 24 is required. Probabilistic tractography has proven to be effective in estimating tract boundaries (Catani et al., 2008; Li et al., 2013; Steele, 2012), and as such lends greater accuracy localizing significant voxels within a given tract. In this study, tractography would have helped verify more precisely in which fibers that voxels with significant FA asymmetry occurred. Another limitation was absence of body mass index data. A body mass index (BMI) could have been included as a covariate, though other research involving ballet dancers reported that lower dancer body mass was not related to FA or GM/WM volume (Hanggi e al., 2010). Finally, the addition of a regional volumetric analysis would have lent greater precision to the current study and improved comparability to other research.

4.3 *Future research*

Future research, currently underway, will report DTI structural parameters including FA, AD, MD, RD and volumetric data (global and regional) in normal, expert (e.g. professional dancers) and Parkinson's disease (PD) patients. Comparing the brain structural characteristics of PD patients and dancers will be the focus of the next phase of study. It will include the DTI structural parameters noted above as well as subcortical volume analysis of the substantial nigra, caudate and putamen. A core trait of PD is disruption of dopaminergic pathways (i.e. the nigrostriatal pathways) and associated structures (substantial nigra, caudate, putamen), which play a critical role in motor control. Moreover, the typical motor control impairment of PD patients is in dramatic contrast to the fluid and highly refined motor control of professional ballet dancers. Historically, contrasts of function and structure among normal, trained, and pathological conditions have greatly informed neuroscience; perhaps the extreme divergence in dancer-PD patient motor control may be reflected in divergent structural brain characteristics, the analysis of which may help further characterize PD brain structure correlates.

***4.4** Conclusion*

We observed that the brain structural metrics of global volume and FA shared relatively large percentages of variability with long-term professional ballet dance training. Dancer training shared 31% of the variability in dancer greater global WM volume (r_s = .55p < .05, r_s^2 = .31); dancer training shared 38% of the variability in dancer greater global GM volume (r_s = .61, p < .01, r_s^2 = .38).

The between group FA findings (i.e. differing FA lateralization and greater FA in dancers) demonstrated similar correlation patterns with AD, MD, and RD. There were no significant correlations between FA lateralization and MD, or between greater FA in dancers and MD. At threshold p < .05 (FWE corrected), there was a strong, positive correlation between FA lateralization and AD but a large negative correlation between FA lateralization and RD. There was an equally strong, positive correlation between greater FA in dancers and AD, but, as with lateralization, also a large negative correlation between greater FA in dancers and RD (p < .10, FWE corrected).

Overall, the FA results of this study were twofold: leftward lateralization in dancers but rightward lateralization in controls, localized to the ATR (p = .038, FWE corrected); greater FA in the CST and SLF of dancers (p = .062, FWE corrected). Both outcomes shared a relatively large percentage of variability with long-term professional ballet dance training. Dancer training shared 55% of the variability (r_s = *.74, p < .001*, r_s^2 = *.55*.) in FA lateralization at the significance level of 0.10 and 30% of the variability (r_s = .55, p < .05, r_s^2 = .30) in FA lateralization at the .05 level of significance. Of note, FA lateralization was negatively correlated with age both at .10 (r_s -.55, p < .05, r_s^2 = .31) and .05 (r_s = -.62, p < .05, r_s =.39), suggesting that FA asymmetry between the groups decreased with progressing age.

Finally, dancer training shared 42% of the variance in the greater (CST/SLF) FA of dancers (r_s =.65, p < .01, r_s^2 =.42). The finding of greater dancer FA in the CST/ SLF tracts positively correlated with AD but negatively correlated with RD implicates enhanced conduction in dancers from altered tract properties, such as increased myelination and possibly increased axon diameter. The increase in AD and

relative decrease of RD in regions of heightened FA is consistent with previous research (Beaulieu, 2002), and in dancers is likely to be related to refined motor control; a beneficial neuroplastic response attending training-induced greater axonal capacity to relay action potentials and communicate (Fields, 2005). Although variation in a structural metric such as FA can stem from any number of factors including genetic predisposition, the relatively high variability shared by years of experience and FA alterations in dancers implicates a substantive effect of training on brain structure.

References

Alexander, D. C. (2005). Maximum entropy spherical deconvolution for diffusion MRI. *Inf Process Med Imaging, 18*

Andrews-Hanna, J. R., Snyder, A. Z., Vincent, J. L., Lustig, C., Head, D., Raichle, M. E., & Buckner, R. L. (2007). Disruption of large-scale brain systems in advanced aging. *Neuron, 56,* 924-935

Barnett, A. (2009). Theory of Q-ball imaging redux: Implications for fiber tracking. *Magn Reson Med.* Doi:10.1002/mrm.22073

Basser, P. J., Jones, D. K. (2002). Diffusion-tensor, MRI: theory, experimental design and data analysis – a technical review. *NMR in Biomedine, 15,* 456-467

Basser, P., Matiello, J., Le Bihan, D. (1994). Estimation of the effective self-diffusion tensor from the NMR spin echo. *J. Magn. Reson., B 103*, 247-254

Beaulieu, C. (2002). The basis of anisotropic water diffusion in the nervous system—a technical review. *NMR. Biomed. 15*, 435–455

Behrens, T. E. J., Johansen-Berg, H., Jbabdi, S., Rushworth, M. F. S., & Woolrich, M.W. (2007). Probabilistic diffusion tractography with multiple fibre orientations. What can we gain? *NeuroImage, 23*:144-155.

Bengtsson, S. L., Nagy, Z., Skare, S., Forsman, L., Forssberg, S., & Ullen, F. (2005). Extensive piano practicing has regionally specific effects on white matter development. Nature *Neuroscience, 8*. doi:10.1038/nn1516

Berthier, M. L., Ralph, M. A. L., Pujol, J., & Green, C. (2012). Arucuate fasciculus variability and repetition: the left sometimes can be right. *Cortex, 48*; 133-143

Boyke J, Driemeyer J, Gaser C, Büchel C, May A. 2008. Traininginduced brain structure changes in the elderly. *J Neurosci. 28,* 7031–7035.

Catani, M., Jones, D. K., & ffytche, D. H. (2005). Perisylvian language networks of the human brain. *Ann Neurol, 57*, 8 –16

Catani, M., Allin, M. P., Husain, M., Pugliese, L., Mesulam, M., Murray, R. M., Jones, D. K. (2007). Symmetries in human brain language pathways correlate with verbal recall. *Proc Natl Acad Sci, 104*, 17163–17168.

Catani, M., & de Schotten, M. T. (2008). A diffusion tensor imaging tractography atlas for virtual in vivo dissections. *Cortex 44*, 1105-1132

Caverzasi, E., Papinutto, N., Amirbekian, B., Berger, M. S., & Henry, R. G (2014). Q-Ball of the Inferior fronto-occipital fasciculus and beyond. *PLOS ONE, 9*, 6, e100272

Cercignani, M., Inglese, M., Pagani, E., Comi, G., Filippi, M., (2001). Mean diffusivity and fractional anisotropy histograms of patients with multiple sclerosis. *Am. J. Neuroradiol. 22*, 952–958.

de Groot, M., Vernooij, M. W., Klein, S., Leemans, A., de Boer, R., van derLugt, A., Breteler, M. M., Niessen, W. J. (2009). Iterative co-linearity filtering and parameterization of fiber tracts in the entire cingulum. *Med Image Comput Comput Assist Interv 12*,853–860.

Colcombe, S. J., Erickson, K. I., Scalf, P. E., Kim, J. S., Prakash, M. E., McAuley, E., … Kramer, A. F. (2006). Aerobic exercise training increases brain volume in aging humans. *Journal of Gerontology, 61A*, 1166-1170

Damasio, A. R., & Geschwind, N. (1984). The neural basis of language. Ann. Rev. *Neurosci, 7*, 127-47

Draganski B, Gaser C, Busch V, Schuierer G, Bogdahn U, May A. (2004). Neuroplasticity: changes in grey matter induced by training. *Nature. 427*, 311–312.

Epstein-Peterson, Z., Faria, A. V., Mori, S., Hillis, & A. E., Tsapkini, K. (2012). Relatively normal repetition performance occurs despite severe disruption of the left arcuate fasciclus. (Neurocase, 18, 521-526

Fields, D., R. (2005). Mylination: an overlooked mechanism of synaptic plasticity. *Neuroscientist, 11(6)*, 528–531.

Fujiwara, H., Namiki, C., Hirao, K., Miyata, J., Shimizu, M., Fukuyama, H., Sawamoto, N., Hayashi, T., Murai, T. (2007). Anterior and posterior cingulum abnormalities and their association

with psychopathology in schizophrenia: a diffusion tensor imaging study. *Schizophr Res 95*, 215–222.

Gannon, P. J., Holloway, R. R., Broadfield, D. C., & Braun A. R. (1998). Asymmetry of the chimpanzee planum temporale: human-like pattern of Wernicke's brain language area homologue. *Science, 279*

Geschwind, N. (1970). The organization of language and the brain. *Science*, 170:940-4

Geschwind, N., & Levisky, W. (1968). Human brain: left right asymmetries in temporal speech region. *Science, New Series, 161*, 186-187

Giorgio, A., Santelli, L., Tommassini, V., Bosenell, R., Smith, S., De Stefano, N., & Johansen-Berg, H. (2010). Age-related changes in grey and white matter structure throughout adulthood. *Neuroimage, 51*, 943-951

Halwani, G. F., Loui, P., Ruber, T., & Schlaug, G. (2011). Effects of practice and experience on the arcuate fasciculus: comparing singers, instrumentalists, and non-musicians. *Frontiers in Psychology, 2*, 156. doi: 10.3389/fpsyg.2011.00156

Hanggi, J., Koeneke, S., Bezzola, L., & Jancke, L. (2010). Structural neuroplasticity in the sensorimotor network of professional female ballet dancers. *Human Brain Mapping, 31*, 1196–1206

Holmes, A.P., Blair, R.C., Watson, J.D., Ford, I. (1996). Nonparametric analysis of statistic images from functional mapping experiments. *J. Cereb. Blood Flow Metab. 16 (1)*, 7–22.

Horsfield, M. (1999). Mapping eddy current induce field for the correction of diffusion weighted echo planar images. *Magentic Resonance Imaging, 17*, 1335-1345.

Horsfield, M., & Jones, D. (2002). Application of diffusion weighted and diffusion tensor MRI to white matter diseases. NMR Biomed, 15, 570-577.

Huettel, A. S., Song, A. W., McCarthy, G. (2009). Functional magnetic resonance imaging, 2nd edition. Sinauer Associates, MA, USA.

Hüfner K, Binetti C, Hamilton D. A., Stephan T, Flanagin V. L, Linn J, Labudda… Brandt, T (2011). Structural and functional plasticity of the hippocampal formation in professional dancers and slackliners. Hippocampus. *21(8),* 855–865.

Kennedy, D.N., O'Craven, K.M., Ticho, B.S., Goldstein, A.M., Makris, N., Henson, J.W. (1999). Structural and functional brain asymmetries in human situs inversus totalis. *Neurology 53 (6),* 1260– 1265

Kheradmand, A., Lasker, A., & Zee, D. S. (2013). Transcranial magnetic stimulation (TMS) of the supramarginal gyrus: A window to perception of upright. *Cerebral Cortex.* doi:10.1093/cercor/bht267

Kahle, W., Platzer, W., Frotscher, M., Leonhardt, H. (2002). Color Atlas and Textbook of Human Anatomy. Thieme, Medical Publishers, Inc., New York.

Kohn, S., E. (1992). Conduction Aphasia. Lawrence Erlbaum Associated, 1992.

Kubicki, M., Westin, C-F., Nestor, P. G., Wible, C. G, Frumin, M., . . . Shenton, M. E. (2003). Cingulate fasciculus integrity disruption in schizophrenia: A magnetic resonance diffusion tensor imaging study. *Biol Psychiatry, 54*:1171–1180

Lebel, C., Beaulieu, C. (2009). Lateralization of the arcuate fasciculus from childhood to adulthood and its relation to cognitive abilities in children. *Hum Brain Mapp 30*, 3563–3573.

Lilliefors, H. (1967). On the Kolmogorov-Smirnov test for normality with mean and variance unknown. *J. Am. Stat. Asscoc., 62,* 399-402

Lim, K., Helpern, J. (2002). Neuropsychic applications of DTI-a review. *NMR Biomed, 15*, 587-593

Madden, D. J., Whiting, W. L., Huettel, S. A., White, L. E., MacFall, J. R., & Provenzale, J. M. (2004). Diffusion tensor imaging of adult age differences in cerebral white matter; relation to response time. *Neuroimage, 21,* 1174-1181.

Maguire, E. A., Gadian, D. G., Johnsrude, I. S., Good, C. D., Ashburner, J., Frackowiack, R. S. J., Frith. C. D. (2000). Navigation-related structural change in the hippocampi of taxi drivers. PNAS, 97, 8

McGill, R., Tukey, J. W., & Larsen, W. A. (February 1978). Variations of box plots. *The American Statistician ,32*, 12–16.

Makris, N., Kennedy, D. N., McInerney, Sorensen, G. A., Wang, R., Caviness Jr., V., S., & Pandya, D., N. (2005). Segmentation of subcomponents within the superior longitudinal fascicle in humans: a quantitative, in vivo, DT-MRI study. *Cerebral Cortex, 15*, 854-869

Mamah, D., Conturo, T. E., Harms, M. P., Akbudak, E., Wang, L., McMichael, A. R., … Csernansky, J. G. (2010). Anterior thalamic radiation integrity in schizophrenia: a diffusion tensor imaging study. *Neuroimaging, 183*, 144-150

May, A. (2010). Experience-dependent structural plasticity in the adult human brain. *Trends in Cognitive Science, 996*

Moseley, M., Cohen, Y., Kucharaczyj, M., Mintorovitch, J., Asgari, H., Wendland, M., Tsuruda, J., & Norman, D. (1990). Diffusion weighted MR imaging of anisotropic water diffusion in cat central nervous system. *Radiology 176*, 439-445

Neil, J., Milner, P., Mukherjee, P., Huppi, P. (2002). Diffusion tensor imaging of normal and injured developing human brain- a technical review. *NMR Biomed, 15*, 543-552

Nichols TE, Holmes AP (2002) Nonparametric permutation tests for functional neuroimaging: primer with examples. Hum Brain Mapp 15:1–25.

Nigmatullina, Y., Hellyer, P. J., Nachev, P., Sharp, D. J., & Seemungal, B. M. (2013). The neuroanatomical correlates of training-related perceptuo-reflex uncoupling in dancers. *Cerebral Cortex*. doi:10.1093/cercor/bht266

Özarslan, E., & Mareci, T. H.(2003). Generalized diffusion tensor imaging and analytical relationships between diffusion tensor imaging and high angular resolution diffusion imaging. *Magn Reson Med, 50*: 955–965

Özarslan, E., Shepherd, T. M., Vemuri, B.C., Blackband. S.J., & Mareci, T. H. (2006). Resolution of complex tissue microarchitecture using the diffusion orientation transform (DOT). *NeuroImage, 31*, 1086–110319

Paparounas, K., Eftaxias D, & Akritidis, N. (2002). Dissociated crossed aphasia: a challenging language representation disorder. *Neurology, 59*:441–2

Pierpaoli, P., Basser, P., 1996. Toward a quantitive assessment of diffusion anisotropy. *Magn. Reson. Med. 36,* 893–906

Pagani, E., Filippi, M., Rocca, M., & Horsfield, M. (2005). A method for obtaining tract-specific diffusion tenor MRI measurements in the presence of disease: application to patients with clinically isolated syndromes suggestive of multiple sclerosis. *Neuroimage 26,* 258-265

Park H. J., Westin, C. F., Kubicki, M., Maier, S. E., Niznikiewicz, M., Baer, A., Frumin, M., Kikinis, R., Jolesz, F. A., McCarley, R. W., & Shenton ME (2004). White matter hemisphere asymmetries in healthy subjects and in schizophrenia: a diffusion tensor MRI study. *Neuroimage 23,* 213–223.

Pascual-Leone, A., Amedi, A., Fregni, F., & Merabet, L. B. (2005). The plastic human cortex. *Annu. Rev. Neurosci, 28,* 377-401

Patel, R., Spreng, R., N., & Turner, G. R. (2013). Functional brain changes following cognitive and motor Skills training: A quantitative meta-analysis. *Neurorehabilitation and Neural Repair, 27,* 187-199

Perlaki, G., Horvath, R., Orsi, G., Aradi, M., Auer, T., Varga, K., … Janszky, J. (2013). White-matter microstructure and language lateralization in left-handers: A whole-brain MRI analaysis. *Brain and Cognition, 83,* 319-328

Powell, H. W., Parker, G. J., Alexander, D.C., Symms, M. R., Boulby, P.A. , Wheeler-Kingshott, C. A., … Duncan, J. S.(2006). Hemispheric asymmetries in language-related pathways: a combined functional MRI and tractography study. *Neuroimage, 32*:388–399

Quigg, M., Fountain, N. B. (1999). Conduction aphasia elicited by stimulation of the left posterior superior temporal gyrus. *J Neurol Neurosurg Psychiatry, 66*:393–6.

Quigg, M., Geldmacher, D. S., Elias, W.J. (2006). Conduction aphasia as a function of the dominant posterior perisylvian cortex. Report of two cases. *J Neurosurg,104*:845–8

R Development Core Team (2008). R: A language and environment for statistical computing. R Foundation for Statistical Computing, Vienna, Austria. ISBN 3-900051-07-0, URL http://www.R-project.org.

Rizzolatti, G., & Craighero, L. (2004). The mirror-neuron system. *Annu. Rev. Neurosci, 27,* 169–92

Rocca, M. A., Valsasina, P., Ceccarelli, A., Absinta, M., Ghezzi, A., Riccitelli, G., Pagani, E., …Filippi, M. (2009) Structural and functional MRI correlates of Stroop control in benign MS. *Hum Brain Mapp 30:*276–290.

Rudrauf, D., Mehta, S., & J. Grabowski,T. J. (2007). Disconnection's renaissance takes shape: Formal incorporation in group-level lesion studies. *Cortex, 44,* 1084-1096

Schefft, B. K, Yeh, H. S., Privitera, M. D., Cahill, W.T., Houston, W. (1995). Repetition and the arcuate fasciculus. *J Neurol, 242*:596–8

Shuren, J. E., Schefft, B. E., Yeh, H., Priviteria, M. D., Cahill, W. T., & Houston, W. (1995). Repetition and the arcuate fasciculus. *J Neurol, 242,* 596-598

Smith, S., M., Jenkinson, M., Woolrich, M.W., Beckmann, C.F., Behrens, T.E.J., Johansen-Berg, H., Bannister, P.R., … Matthews, P.M. (2004). Advances in functional and structural MR image analysis and implementation as FSL. *NeuroImage, 23(S1),* 208-219

Song, S. K., Yoshino, J., Le, T.Q., Lin, S. J., Sun, S. W., Cross, A. H., Armstrong, R. C. (2005). Demyelination increases radial diffusivity in corpus callosum of mouse brain. *NeuroImage, 2*6:132–140

Sotiropoulus, S., Anderson, J. Retrieved April 15, 2014, from http://fsl.fmrib.ox.ac.uk/fslcourse/lectures/fdt1.pdf

Sowell, E. R., Thompson, P. M., Rex, D., Kornsand, D., Tessner, K. D., Jernigan, T. L., & Toga, A. W. (2002). Mapping sulcal pattern asymmetry and local cortical surface gray matter distribution in vivo: maturation in perisylvian cortices. *Cerebral Cortex, 12,* 17-26

Steele, C. J. (2012). The relationship between brain, structure motor performance, and early musical training. Unpublished manuscript.

Strenziok, M., Greenwood, P. M., Santa Cruz, S. A., Thompson, J. C., Parasuraman, R. (2013). Differential contributions of dorso-ventral and postro-caudal prefrontal white matter tracts to cognitive control in healthy older adults. *PLOS ONE, 8,* 12, e81410

Taubert, M, Draganski, B, Anwander, A, Müller, K, Horstmann, A, Villringer, A, Ragert P. (2010). Dynamic properties of human brain structure:learning-related changes in cortical areas and associated fiber connections. J Neurosci. 30(35):11670–11677.

Takao, H., Hayashi, N., Tohomo, K. (2011). White matter asymmetry in healthy individuals: a diffusion tensor imaging study using tract-based spatial statistics. *Neuroscience,193,* 291–299

Takeuchi, H., Yamanouchi T., Sekiguchi, A., Suzuki, S., Taki, Y., Kawashima, R. (2010). Training of Working Memory Impacts Structural Connectivity. *The Journal of Neuroscience. 30,* 3297-33

Tuch, D. S. (2002). Diffusion MRI of complex tissue structure. Ph.D. thesis. Massachusetts Institute of Technology.

Tuch, D. S. (2004). Q-Ball imaging." *Magnetic Resonance in Medicine*, *52*, 1358-1372.

Tuch, D. S., Weisskoff, R. M., Belliveau, J.W., Wedeen, V. J. (1999). High angular resolution diffusion imaging of the human brain. In: Proceedings of the 7th Annual Meeting of ISMRM, Philadelphia, p 321

Upadhyay, J., Hallock, K., Ducros. M., Kim, D. S., Ronen, I. (2008). Diffusion tensor spectroscopy and imaging of the arcuate fasciculus. *Neuroimage 39*, 1–9.

Wakana, S., Caprihan, A., Panzenboeck, M. M., Fallon, J.H., Perry, M., Gollub, R. L., Hua, K, Zhang, J, … & Mori, S. (2007). Reproducibility of quantitative tractography methods applied to cerebral white matter. *Neuroimage 36*, 630–644.

Wang, B., Fan, Y., Lu, M., Shumei Li, S., Zheng Song, Z., Peng, X., Lin, Q., … Zhang, R. (2013). Brain anatomical networks in world class gymnasts: a DTI tractography study. *NeuroImage 65*, 476–487

Wedeen, V. J., Hagmann, P, Tseng, W.Y., Reese, T. G., & Weisskoff, R. M. (2005). Mapping complex tissue architecture with diffusion spectrum magnetic resonance imaging. *Magn Reson Med 2005, 54*: 1377–1386

Wernicke, C. (1874). The aphasic symptom complex: a psychological study on a neurological basis. *Boston Stud Philos Sci, 4*

Winkler, A. M., Ridgway, G. R., Webster, M. A., Smith, M. S., Nichols, T. E. (2014). Permutation inference for the general linear model. *NeuroImage, prepress*

Appendix A

Table1. Fractional anisotropy

Dancer L >0 FA

Voxels	Max X (mm)	Max Y (mm)	Max Z (mm)	L>0, JHU-ICBM	*p* <.10
538	-30	41	-3	5% IFOF; 3% ATR	0.0372
272	-17	53	12	58% Fmi; 5% Ci; 3% IFOF; 3% ATR	0.0567
179	-29	30	24	3% UN; 3% IFOF; 3% ATR	0.0313
88	-13	-93	9	18% Fma; 5% IFOF; 3% ILF	0.0567
69	-28	0	29	3% SLF (temporal); 3% SLF	0.0469
48	-24	-66	1	8% ILF; 8% IFOF; 3% Fma	0.0508
46	-32	-1	-26	18% IFOF	0.0377
41	-25	-67	13	37% Fma	0.0040
33	-36	-24	27	63% SLF; 32% SLF (temporal)	0.0469
28	-17	47	-10	19% UN; 18% IFOF; 8% ATR; 5% Fmi; 3% SLF	0.0566
25	-21	23	-2	50% IFOF; 36% UN; 18% ATR	0.0371
18	-34	-11	-15	5% ATR; 3% IFOF	0.0566
11	-22	-82	2	42% Fma; 16% ILF; 11% IFOF	0.0566
8	-28	4	26	**3% SLF (temporal); 3% SLF**	0.0977
8	-31	-65	1	53% IFOF; 24% ILF; 5% Fma	0.0859
7	-24	23	11	37% IFOF; 19% UN; 11% ATR; 3% SLF	0.0957
6	-15	-12	17	11% ATR	0.0645
4	-25	32	9	32% ATR; 29% IFOF; 19% UN	0.0899
3	-10	-61	26	5% Ci	0.0821
3	-24	-54	23	3% IFOF; 3% FMa; 3% ATR	0.0469
3	-9	-85	23	8% FMa; 3% Ci	0.0703
3	-25	31	12	34% IFOF; 29% ATR; 17% UN	0.0899
3	-23	21	6	51% IFOF; 21% ATR	0.0977
2	-14	-17	15	11% ATR	0.0469
2	-23	18	14	50% ATR; 5% IFOF	0.0957
2	-24	-47	3	no label found	0.0899
1	-8	26	23	19 % Ci	0.0977
1	-24	-79	1	45% FMa; 21% IFOF; 18 % ILF	0.0997
1	-27	-57	0	6% Ci; 3% IFOF	0.0977
1	-35	4	20	**21% SLF: 13% SLF (temporal part)**	0.0664

AF= arcuate fasciculus; ATR = anterior thalamic radiation; Ci = cingulum; forceps major= FMa; FMi = forceps minor; IFOF = inferior fronto-occiptal fasciculus; ILF = inferior longitudinal fasciculus; SLF = superior longitudinal fasciculus; UF = uncinate fasciculus. JHU- ICBM White-Matter percentages represent the probability that significant fractional anisotropy (FA) occurs in the associated structure.

Table 2

Controls L>0 FA

Voxels	Max X (mm)	Max Y (mm)	Max Z (mm)	L>0, JHU-ICBM	*p* <.10
387	-28	2	-11	6% UN; 3% IFOF	0.043
183	-32	36	-1	11% UN; 8% IFOF	0.035
143	-20	23	-5	45% IFOF; 33% UN; 5% ATR; 3% SLF (temporal part)	0.006
59	-15	-21	14	no label found	0.048
47	-27	14	28	no label found	0.068
46	-28	39	17	5% ATR	0.082
43	-14	-53	23	3% Ci (posterior)	0.033
31	-25	-12	34	3% SLF; 3% CST	0.068
19	-25	34	7	37% IFOFl; 37% ATR; 22% UN; 3% SLF	0.068
15	-30	-2	-30	3% ILF; 3% Ci	0.092
14	-2	-38	-34	3% ATR	0.018
9	-17	8	-15	no label found	0.076
5	-24	31	12	50% ATR; 24% IFOF; 8% UN; 3% SLF	0.088
4	-24	-4	34	5% SLF	0.092
4	-29	30	25	3% IFOF; 3% ATR	0.098
2	-21	-52	22	5% Fma	0.086
2	-10	-1	11	26% ATR	0.018
2	-29	42	8	11% ATR; 5% IFOF; 3% UN	0.098
1	-31	43	8	8% ATR; 3% IFOF; 3% Fmi	0.100
1	-32	45	2	11% ATR; 3% UN; 3% IFOF	0.098

AF= arcuate fasciculus; ATR = anterior thalamic radiation; Ci = cingulum; CST= cortical spinal tract; forceps major= FMa; FMi = forceps minor; IFOF = inferior fronto-occiptal fasciculus; ILF = inferior longitudinal fasciculus; SLF = superior longitudinal fasciculus; UF = uncinate fasciculus. JHU- ICBM White-Matter percentages represent the probability that significant fractional anisotropy (FA) occurs in the associated structure